AD-A118 584 NAVAL RESEARCH LAB WASHINGTON DC F/G 9/5

CALCULATION OF COSMIC-RAY INDUCED SOFT UPSETS AND SCALING IN VL--ETC(U)

AUG 82 P SHAPIRO, E L PETERSEN, J H ADAMS

UNCLASSIFIED NRL-MR-4864 NL

END

DATE FILMED

9 82

DTIC

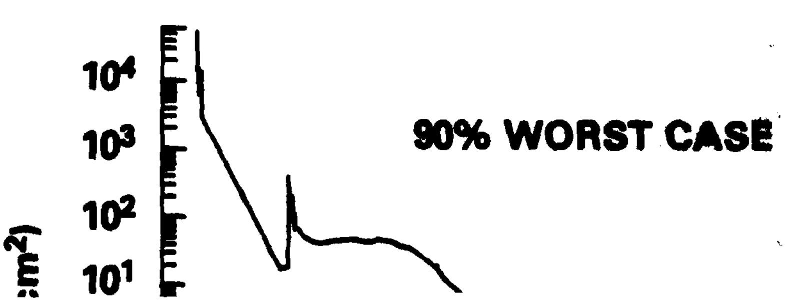
10^4
10^3
10^2
10^1
:m²)
90% WORST CASE

SECURITY CLASSIFICATION OF THIS PAGE (When Data Entered)

REPORT DOCUMENTATION PAGE

READ INSTRUCTIONS BEFORE COMPLETING FORM

1. REPORT NUMBER NRL Memorandum Report 4864	2. GOVT ACCESSION NO. AD-A118584	3. RECIPIENT'S CATALOG NUMBER
4. TITLE (and Subtitle) CALCULATION OF COSMIC-RAY INDUCED SOFT UPSETS AND SCALING IN VLSI DEVICES		5. TYPE OF REPORT & PERIOD COVERED Interim report on a continuing NRL problem. 6. PERFORMING ORG. REPORT NUMBER
7. AUTHOR(s) P. Shapiro, E.L. Petersen, and J.H. Adams, Jr.		8. CONTRACT OR GRANT NUMBER(s)
9. PERFORMING ORGANIZATION NAME AND ADDRESS Naval Research Laboratory Washington, DC 20375		10. PROGRAM ELEMENT, PROJECT, TASK AREA & WORK UNIT NUMBERS 62712N; XF12141310; 66-0469-0-2; 62715H; X99QAXVB; 66-0449-0-2
11. CONTROLLING OFFICE NAME AND ADDRESS Naval Electronics Systems Command, Washington, DC 20360 Defense Nuclear Agency, Washington, DC 20305		12. REPORT DATE August 26, 1982 13. NUMBER OF PAGES 42
14. MONITORING AGENCY NAME & ADDRESS(if different from Controlling Office)		15. SECURITY CLASS. (of this report) UNCLASSIFIED 15a. DECLASSIFICATION/DOWNGRADING SCHEDULE

16. DISTRIBUTION STATEMENT (of this Report)

Approved for public release; distribution unlimited.

17. DISTRIBUTION STATEMENT (of the abstract entered in Block 20, if different from Report)

18. SUPPLEMENTARY NOTES

This work was partially sponsored by the Defense Nuclear Agency under Subtask X99QAXVB, work unit 00017, work unit title "Single Events Experiments," and by the Naval Electronic Systems Command.

19. KEY WORDS (Continue on reverse side if necessary and identify by block number)

Cosmic rays	Soft upsets	Microdosimetry
Radiation belts	Single-event upsets	VHSIC
Microelectronics	Chord-length distributions	Spacecraft electronics
Soft errors	VLSI	

20. ABSTRACT (Continue on reverse side if necessary and identify by block number)

An analysis was carried out to explore the effect of size reduction on cosmic-ray induced errors in RAM's. This analysis uses a computational model and scaling procedure that are representative of those reported in current literature. Availability of various cosmic-ray environments make it possible to examine the effect of variations in the environment on predicted soft-upset rates. In addition, soft-upset rates have been calculated for the direct ionization due to protons in the radiation belts at an altitude of 600 nautical miles.

DD FORM 1 JAN 73 1473 EDITION OF 1 NOV 65 IS OBSOLETE
S/N 0102-014-6601

SECURITY CLASSIFICATION OF THIS PAGE (When Data Entered)

CONTENTS

CALCULATION OF COSMIC-RAY INDUCED
SOFT UPSETS AND SCALING IN VLSI DEVICES

I. INTRODUCTION

Progression of VLSI (Very Large Scale Integration) circuitry to smaller feature sizes substantially increases the probability of soft upsets induced by the penetration of energetic cosmic-ray particles through the device.[1] These devices can change their logic state without permanent damage to the device when a densely-ionizing particle deposits a quantity of charge at a node (an MOS capacitor, for example) that is comparable to the quantity of charge representing the logic state.

An exploratory study is needed at this time to estimate the effect of scaling of microelectronic devices to smaller sizes on expected soft-upset rates in the cosmic ray environments encountered by satellites. A definitive calculation requires knowledge of the way microelectronic technology will proceed on scaling to smaller feature sizes. However, some limiting cases can be studied which will indicate whether soft-upset rates become impossibly large on further scaling or whether tolerable soft-upset rates are to be anticipated as we evolve to the VHSIC (very high speed integrated circuit) era. Such an exploratory calculation has been carried out by Burke.[2] The calculations reported herein are an extension of the Burke calculations in that our calculations are based on extended cosmic-ray environments recently developed by the NRL Laboratory for Cosmic Ray Physics,[3] and our calculations employ exact evaluation of the integral chord-length distributions. Scaling of the device structures is extended to feature sizes of approximately 0.1 micrometer, and variation in the scaling laws is explored.

The study by Burke parametrizes a cosmic-ray LET spectrum generated by Heinrich.[4] The Heinrich spectrum only includes cosmic-ray components with $6 \leq Z \leq 26$, whereas the NRL spectrum includes a larger range of Z, $1 \leq Z \leq 28$. In addition, the NRL analysis accounts for temporal variations by producing data for three cosmic ray environments: solar maximum activity, solar minimum activity, and a 90 percent worst case condition. The 90 percent worst case is the environment most reasonable to use in reliability studies for satellite-borne electronics since this level of solar activity, by definition, will only be exceeded 10 percent of the time. In addition, soft-upset rates have been calculated for the direct ionization due to protons in the radiation belts at an altitude of 600 nautical miles. The contribution to soft-upset rates by proton-induced nuclear reactions is the subject of a continuing investigation. The present calculations illustrate the dependence of expected soft-upset rates on environment.

Manuscript submitted June 4, 1982.

Exact evaluation of the integral chord length distributions and comparison with approximate expressions which have been used by others are shown for selected examples.

Evaluation of soft upset rates for the same random access memories (RAMs) that have been studied by Burke has been performed using the same geometrical parameters and critical energies in order to facilitate comparison.

II. ENVIRONMENTS

The LET spectra for the cosmic-ray environments were derived from the work of Adams et al.[3] We considered the pure galactic cosmic ray environment at times of minimum and maximum solar activity. The LET spectra for these two environments are shown in Figures 1 and 2 respectively. For the 90 percent worst case spectrum, we have included a 90 percent worst case contribution of low energy particles from solar and interplanetary activity in addition to galactic cosmic rays as they appear during the period of minimum solar activity. Only 10 percent of the time should conditions in the interplanetary medium be more hostile for microelectronic components. This 90 percent worst case spectrum, of extreme importance for estimation of satellite vulnerability, is shown in Figure 3.

A copy of the LET spectrum for cosmic rays due to Heinrich[4] is shown for reference in Figure 4. This LET spectrum is very close to the solar maximum spectrum generated at NRL.

Figure 5 shows the LET spectrum for protons for a 600 nautical mile orbit in the proton radiation belts. The proton spectrum[5] was obtained by using the radiation belt proton spectrum of AP8-MAX[6] integrated over a 63° 1111 km orbit, and allowing for the shielding of a typical light spacecraft. The proton energy spectrum was converted to an LET spectrum using the tables of Williamson and Boujot.[7] This spectrum includes only the direct ionization effects of the protons, and does not include the ionization of any reaction products. As pointed out in references 5 and 8, the proton reaction products can easily produce upsets in unscaled NMOS devices, so that the actual upset rates are much higher at large scaling factors than given by predictions using this spectrum. This curve is useful for showing the worst case upset rates as scaled devices become sensitive to the direct ionization.

III. DISCUSSION OF CALCULATION

A. Soft Upset Calculation

Techniques originally developed in the field of microdosimetry are utilized in calculation of expected soft upset rates. In a pioneering work, Bradford[9] has shown how to use the studies of Kellerer on the problem of random traversals of convex bodies by straight lines for the calculation of expected soft-upset rates. The presentation of the Bradford theory given here closely follows that of Burke.[2] In this model, the sensitive volume

of a MOS capacitor in a random access memory is represented by a [illegible] parallelepiped with dimensions a, b, c, where $a \leq b \leq c$, [illegible] calculate the probability that a cosmic-ray particle passing through the sensitive volume will create enough ionization along its path to change the logic state of the device. It is assumed that the funnel effect[10] does not occur, i.e., that only charge deposited in the oxide layer of the MOS device actually contributes to the collected charge. NRL experiments on MOS and diffused junction test structures[11] indicate that MOS devices collect significantly less charge from the same particle than diffused junction devices. The energy deposited, E_{dep}, is given by

$$E_{dep} = L\rho\ell, \tag{1}$$

where L is the linear-energy transfer for the particle (LET), ρ is the density of the material, and ℓ is the chord length for the particular traversal through the sensitive volume. The number of electron-hole pairs created is E_{dep}/E_{e-h}, where E_{e-h} is the energy required to create an electron-hole pair, 3.6 eV in the case of Si. When E_{dep} is greater than ΔE, a critical energy, a sufficient number of electron-hole pairs is created to cause an event. Thus, an event can occur if the chord length associated with the particular passage of a particle is greater than ℓ_{min}, where

$$\ell_{min} = \Delta E/\rho L. \tag{2}$$

It is shown by Kellerer,[12] that in an isotropic uniform field of fluence ϕ, the expected number of chords through a convex body of surface S is $S\phi/4$. If this number is multiplied by $C(\ell_{min})$, the sum probability that the chord-length through the sensitive volume is greater than ℓ_{min}, N_e, the number of events that deposit an energy greater then ΔE is obtained. For a continuous spectrum, N_e is obtained by integration of

$$N_e = \frac{S}{4}\int_{L_o}^{L_{max}} \phi(L)\, C\left(\frac{\Delta E}{\rho L}\right) dL. \tag{3}$$

In this integral, $\phi(L)$ is obtained from $\phi(E)$ using the transformation

$$\phi(L) = \phi(E)\,\frac{dE}{dL}. \tag{4}$$

The ℓ_{min} dependence in $C(\ell_{min})$ has been converted to a dependence on L using equation (2) so that the integration over L can be performed. The lower limit of integration is the minimum value of L than can produce an event,

$$L_o = \Delta E/\rho\ell_{max} \tag{5}$$

where ℓ_{max} is the diagonal of the parallelepiped, i.e.,

$$\ell_{max} = (a^2 + b^2 + c^2)^{1/2}. \tag{6}$$

L_{max} is the maximum value of L included in $\phi(L)$. In the event that the lowest value of L (call it L^*) contained in $\phi(L)$ is larger than L_o, $\phi(L)$ is taken to be zero in the interval, $L_o \le L \le L^*$.

An alternative formulation to calculate N_e which is fully equivalent to equation (3) has been used by Pickel and Blandford.[13] This formulation uses $\Phi(L)$, the integral LET spectrum, and $f(\ell)$, the differential chord-length distribution. These quantities are related to $\phi(L)$ and $C(\ell)$ by

$$\Phi(L) = \int_{L}^{L_{max}} \phi(x)dx. \qquad (7)$$

$$C(\ell) = \int_{\ell}^{\ell_{max}} f(x)dx. \qquad (8)$$

The equivalence of the two formalisms is easily shown by expanding equation (3)

$$N_e = \frac{S}{4} \int_{L_o}^{L_{max}} \phi(L) \int_{\ell}^{\ell_{max}} f(\ell')d\ell' dL, \qquad (9)$$

where $\ell = \frac{\Delta E}{\rho L}$

Interchanging the order of integration, with the appropriate change of limits,we have

$$N_e = \frac{S}{4} \int_{\ell_o}^{\ell_{max}} f(\ell) \int_{L(\ell)}^{L_{max}} \phi(L')dL' d\ell \qquad (10)$$

Here, $L(\ell) = \Delta E/\rho\ell$, the minimum value of LET which will deposit ΔE in the sensitive volume for that value of L, and $\ell_o = \Delta E/\rho L_{max}$. Using (7) above,

$$N_e = \frac{S}{4} \int_{\ell_o}^{\ell_{max}} f(\ell)\Phi[L(\ell)]\, d\ell. \qquad (11)$$

B. Chord-length distributions

Kellerer[12] does not furnish explicit expressions for the chord-length distributions that appear in his theoretical work on

microdosimetry. However, Bradford has utilized an exact result by Coleman[14] for the differential chord-length distribution for a two-dimensional rectangle together with the formalism developed by Kellerer relating the various two- and three-dimensional chord-length distributions to derive an approximate expression for $C(\ell)$, the integral chord-length distribution for a rectangular parallelepiped. The approximation is claimed to be useful for b/a or c/a $\geq$ 3. This approximate evaluation of $C(\ell)$ is very useful since it furnishes an expression for $C(\ell)$ in closed form. Burke, in the worked cited above, has used a further approximation to the Bradford expression which is in a convenient form for hand calculation.[15] This approximation is

$$C(\ell) = 0.75\ (a/\ell)^{2.2} \qquad \ell \geq a \tag{12a}$$

$$C(\ell) = 1\ -0.25\ (\ell/a) \qquad \ell \leq a. \tag{12b}$$

These approximate results are very useful, yielding values of $C(\ell)$ quite close to the exact result except that $C(\ell)$ does not go to zero correctly for large ℓ near ℓ_{max}.

An exact expression for the differential chord-length distribution, $f(\ell)$, due to Petroff is contained in a paper by Pickel and Blandford.[13] We have evaluated $C(\ell)$ by numerical integration of the Petroff result, utilizing equation (8). This exact result for the geometries used in the soft-upset calculations is compared with an evaluation utilizing Bradford's approximation (Approximation 1), and the approximation used by Burke (Approximation 2). We have also compared the Bradford approximation with an exact calculation for a case studied by Ziegler.[16]

Comparisons between the exact calculation of $C(\ell)$ and Approximation 1 are shown in Figures 6 to 9. We note that results are almost identical for small ℓ until the first discontinuity in $C(\ell)$ is reached, and that the results are in quite good agreement beyond that until ℓ reaches a value larger than the last discontinuity in $C(\ell)$. For these larger values of ℓ, Approximation 1 for $C(\ell)$ does not go to zero properly at ℓ_{max}. The examples shown in Figures 6 to 8 satisfy the criterion given by Bradford for the usefulness of the approximate formula. Figure 9 shows a case where the parallelepiped approaches a cube, the case studied by Ziegler. In this case the disagreement at large chord lengths is greater.

Approximation 2 is compared with the exact calculation for $C(\ell)$ in Figures 10 to 12. Again, the results using this approximation are reasonably close to the exact results except for the longer chord lengths. The degree of agreement seems to be dependent on how well the condition b/a $\geq$ 3 is satisfied.

IV. DEVICE SCALING AND CALCULATION OF SOFT-UPSET RATE

A. SCALING

Soft-upset rates in the cosmic-ray environment have been calculated for the particular memory devices studied by Burke.[2] The

scaling scenarios reported by Burke are extended to smaller feature sizes and soft-upset rates are calculated for the various environments discussed in Section II. Furthermore, where equation 3 is utilized to calculate the number of events that deposit energy greater than ΔE by cosmic rays or by direct ionization from protons in the radiation belts, exact evaluation of $C(\ell)$ is employed. When scaling to smaller device size, equation 3 can be considered to apply to the reference devices, 4K memories. It is not clear at this time how the technology will evolve when VLSI devices are scaled down to smaller feature sizes. One scaling scenario that can be considered is scaling according to the model of Mead and Conway.[17] In this model, all of the linear dimensions are reduced by a scaling factor α,

$$a' = a/\alpha \tag{13a}$$
$$b' = b/\alpha \tag{13b}$$
$$c' = c/\alpha \tag{13c}$$

Furthermore, all voltages are scaled down by dividing by the same scaling factor α, thus keeping all electric fields in the device constant. With these assumptions, the stored charge representing a bit scales as α^{-2}. This follows from the fact that the capacitance, C, being proportional to an area divided by a separation distance, scales as α^{-1}. Since $Q = CV$, Q scales as α^{-2}. Critical energy is directly proportional to critical charge, i.e., $\Delta E = \epsilon Q$ where $\epsilon = 3.6$ eV/eh-pair in silicon. Thus the critical energy for upset scales as

$$\Delta E' = \Delta E/\alpha^2. \tag{14}$$

The Mead and Conway scaling scenario is rather simplistic and cannot be expected to apply indefinitely as devices get smaller and smaller. For example, at some point it is not practical to continue reducing the voltage as the signal to noise ratio will become intolerable. Furthermore, the recently-discovered funneling phenomenon[10] will cause the effective charge-collection volume to scale differently than the physical dimensions of the volume storing the charge that represents a bit. Correct scaling would have to take funneling into account as the device dimensions become smaller. At the present time it is not clear which of many possible scaling scenarios should be used for these exploratory calculations. Hence, for part of the analysis of soft-upset rates reported here, a worst-case assumption has been made that ΔE varies as α^{-3}. We have also explored the effect of variation of scaling laws by repeating the calculations for ΔE varying as α^{-2}, probably the most realistic scaling assumption with our present knowledge.

With the assumption that ΔE scales as α^{-3}, and the scaling of linear dimensions at α^{-1}, the minimum chord length, ℓ_{min}, for deposit of energy greater than ΔE, scales as

$$\ell'_{min} = \Delta E/\alpha^3 L. \tag{15}$$

Furthermore, the lower limit of integration L_o scales as

$$L'_o = L_o/\alpha^2. \tag{16}$$

Assuming that the same chip area will be devoted to memory, if the reference size is M, the new size M' is

$$M' = \alpha^2 M. \tag{17}$$

However, the quantity S in equation 3 is the surface per cell so that

$$S' = S/\alpha^2 \tag{18}$$

for the calculation of events per bit-day.

The basic equation for calculation of event-rate after scaling becomes,

$$Ne = S/4\alpha^2 \int_{L_o'}^{L_{max}} \phi(L)C(\Delta E/\alpha^3 \rho L)dL. \tag{19}$$

The error rate, N_E, is obtained by multiplication by ϵ, the error conversion factor.

$$N_E = Ne\ \epsilon. \tag{20}$$

This error conversion factor, ϵ, which depends on the memory configuration, is (number of cells/memory unit) x (vulnerability/cell).

B. EXAMPLES

Application of the preceding theory requires availability of the cell dimensions and critical energy for specific devices. Following Burke, we use the parameters developed by Pickel and Blandford[13,18] for a number of device types. The parameters used in the calculations are listed in Table I.

The critical dimensions for the NMOS dynamic RAM were inferred by Pickel and Blandford from the manufacturer's data on the device. The error conversion factor, ϵ, in equation 20 is set equal to 1/2, assuming ~ 1/2 the cells are empty at one time, as did Pickel and Blandford.

The parameters for a CMOS-Bulk RAM example were also obtained from reference 13. Here the value of ΔE = 22.5 MeV is obtained from heavy-ion upset measurements. In this case, since there are six devices per memory unit and 1/2 are vulnerable, ϵ is set equal to 3.

Similarly, the dimensions for the 4K, CMOS-SOS, five-transistor memory cell RAM's were obtained from the work of Pickel and Blandford. Following the approximation used by Burke, ϵ is set equal to 5 in place of the averaging procedure used by Pickel and Blandford.

The results of calculation of soft-upset rate for the three device types in the 90 percent worst case spectrum environment are presented in

Figure 13. As in all of our calculations, the scaling goes from $\alpha = 0.5$ to $\alpha = 100$, well beyond the VHSIC region. The relative vulnerability of the various devices is indicated. Furthermore we see that as larger scale integration proceeds, the predicted soft-upset rate peaks at the 256K to 1M memory size and then falls off.

The dependence of predicted soft-upset rate on the specific environment is shown in Figures 14 to 16. These results suggest that detailed analysis of the environment associated with a particular satellite orbit improves the predictive accuracy of soft-upset calculations.

The Heinrich spectrum used by Burke in his calculations is very close to the solar maximum spectrum used in the NRL calculations. Although calculations utilizing the solar maximum spectrum yield similar results in the range of scaling explored by Burke, the NRL calculations with the solar minimum spectrum agree more closely with Burke's results. The fact that there is reasonable agreement between the Burke- and the NRL-calculations indicates that the Burke approximation for the chord-length distributions does not introduce any large errors.

The importance of the critical energy parameter, ΔE, is shown in Figure 17. Here, the critical energy has been arbitrarily quadrupled for a calculation of soft upset rate for the N-MOS dynamic RAM. This change in ΔE reduces the vulnerability by approximately an order of magnitude.

The calculations presented up to this point with ΔE proportional to α^{-3} can be considered a worst-case of scaling to smaller device features. The effect of scaling the critical energy as α^{-2} instead of α^{-3} is shown in Figures 18 to 20. It is quite likely that the α^{-2} scaling is more applicable to the way device scaling will go. We note that the α^{-2} scaling predicts soft-upset rates two to three orders of magnitude lower than that predicted for α^{-3} scaling for scale factors larger than 10. This strong dependence of predicted soft-upset rate on scaling scenario indicates that a more detailed investigation of scaling is required for accurate soft-upset rate predictions.

The predicted soft-error rate due to direct ionization by protons in the proton radiation belt at 600 nautical miles is shown in Figures 21 and 22 for the critical energy scaling as α^{-3} and as α^{-2}. These results are preliminary as work is in progress on the soft-upset rate induced by nuclear reactions in silicon.

V. SUMMARY AND DISCUSSION

Calculations of predicted rates of soft-upset failure of devices in the cosmic-ray environment are presented which parallel calculations performed by Burke. The present calculations utilize improved cosmic-ray environments generated at NRL, and exact calculation of the integral chord-length distributions. Furthermore, the scaling is extended to smaller device sizes.

The NRL predictions of soft-upset rate yield similar results to those

obtained by Burke. This agreement indicates that the Burke approximation to the integral chord-length distribution does not introduce large errors.

Calculations utilizing the 90 percent worst case spectrum show a large increase in predicted soft-upset rate in the scaling range of approximately four to eighty over the results of Burke. The 90 percent worst case spectrum is to be preferred for a more realistic estimate of the soft-upset risk for a satellite in the cosmic-ray environment than not including the contribution due to low level solar and interplanetary activity. Comparison of soft-upset rates in the three cosmic-ray environments utilized in these calculations indicates the importance of accurate evaluation of the environment for reliable prediction of soft-upset failure rates.

The variation of predicted soft-upset rate with the critical energy shows the importance of correct determination of the device parameters for soft-upset predictions. A calculation with two different scaling scenarios shows the dependence of soft upset rate on the details of scaling. Clearly, further investigation of scaling is required. Perhaps, it would be more correct to use different scaling scenarios for each of several regions of scaling.

Preliminary results of predicted soft-upset rates in the proton radiation belts at 600 nautical miles are presented. These calculations only include effects due to direct ionization by the protons. Errors due to direct ionization by protons in the radiation belts can become the limiting factor on missions as devices are scaled down. For the examples in the present calculations there is a rapid increase in soft-upset rate at a scaling factor of approximately four. For more sensitive devices, failure rate can become catastrophic with current technologies.

An important conclusion that can be inferred from these exploratory calculations with several scaling scenarios is that cosmic-ray induced soft-upset rates do not increase indefinitely as feature size is scaled down.

VI. ACKNOWLEDGMENTS

We wish to thank E. A. Burke for furnishing us with a manuscript of his Rome Air Development Center Technical Memorandum prior to issuance. This Technical Memorandum stimulated the work reported herein.

The continued support and encouragement of J. C. Ritter during the course of this work is greatly appreciated.

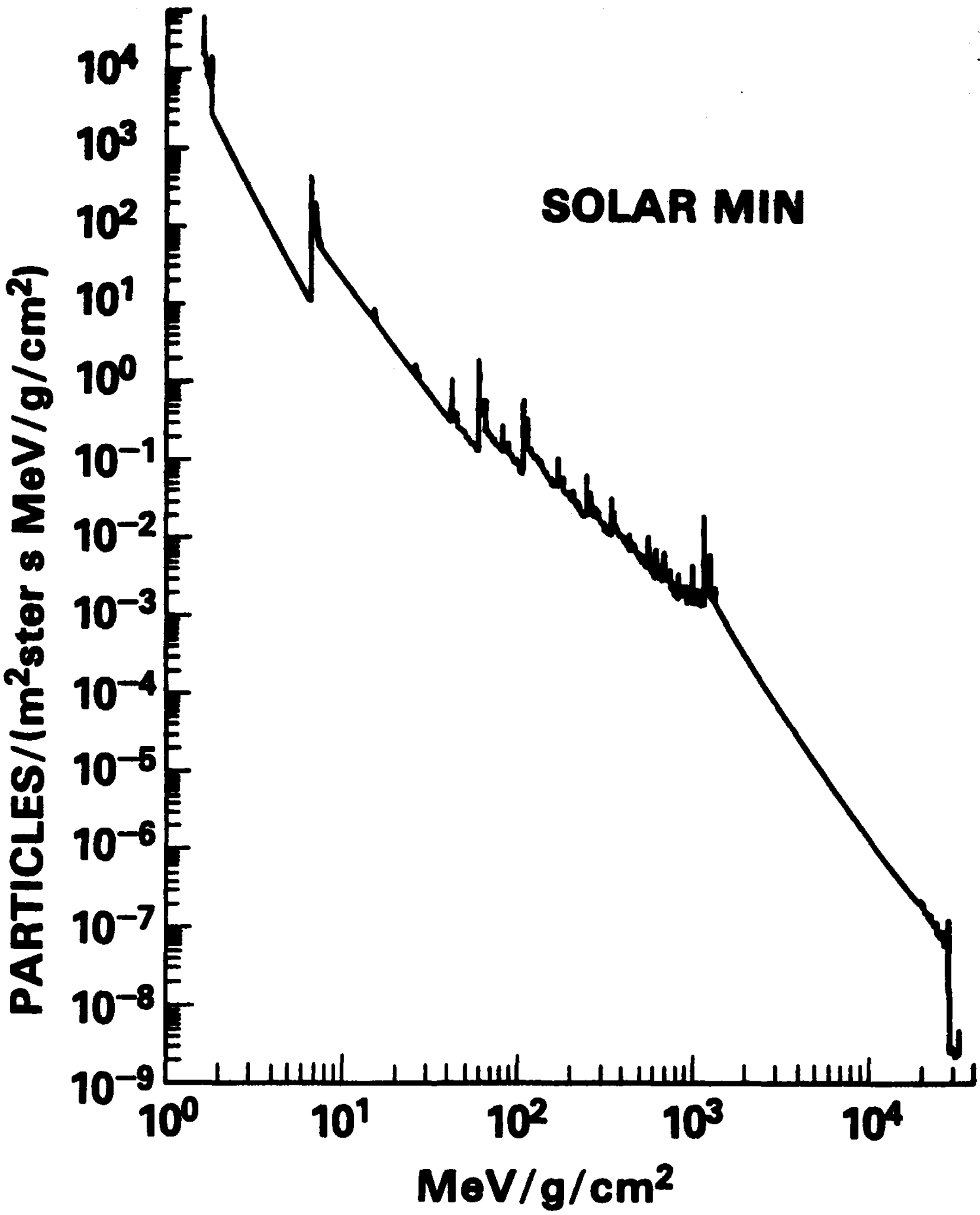

Figure 1. LET spectrum due to galactic cosmic rays at times of minimum solar activity. The spikes in this and the following figures arise from singularities in the conversion from energy to LET spectra. It is the area under these spikes and not their height that carry information on the differential particle flux.

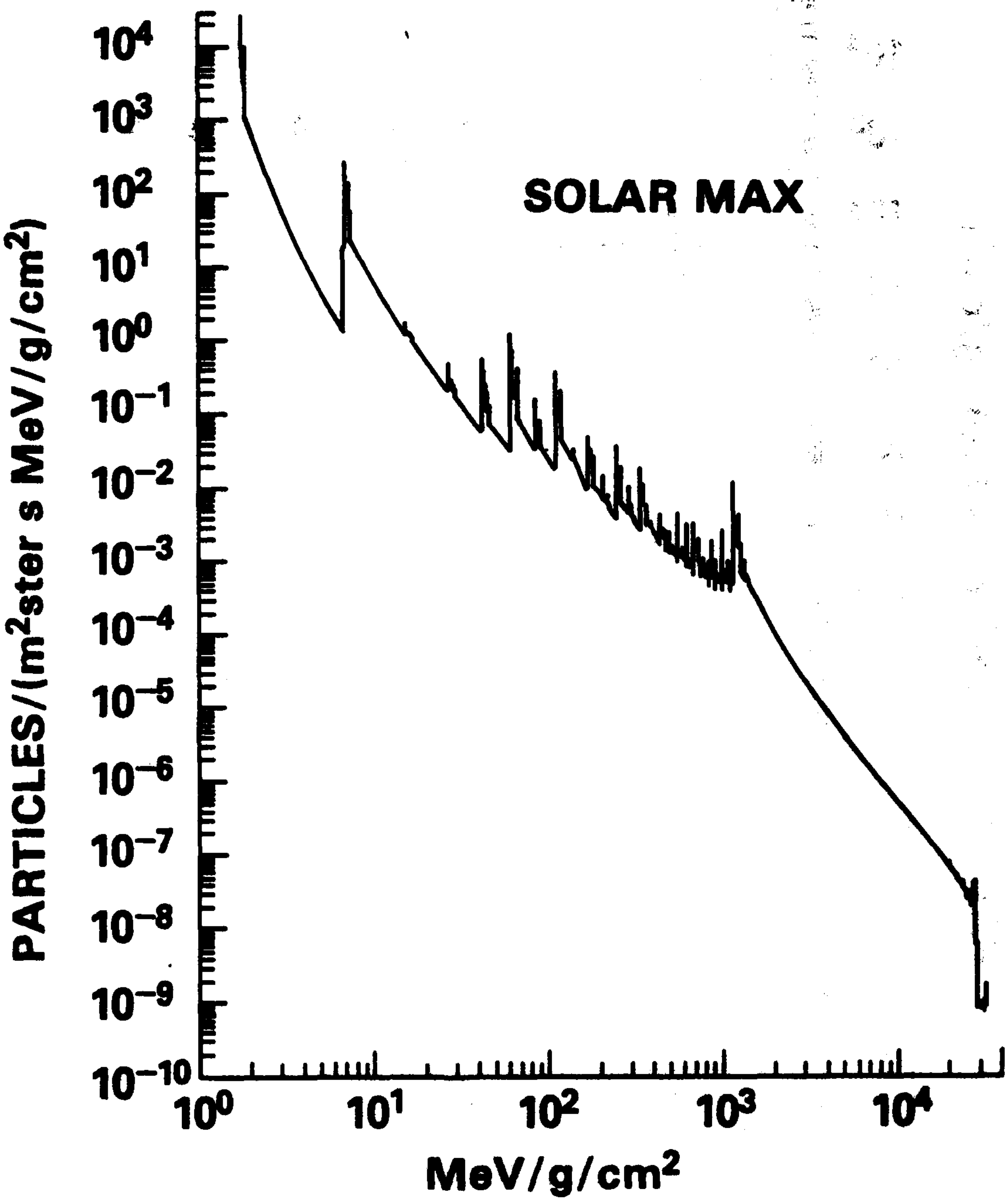

Figure 2. LET spectrum due to galactic cosmic rays at times of maximum solar activity.

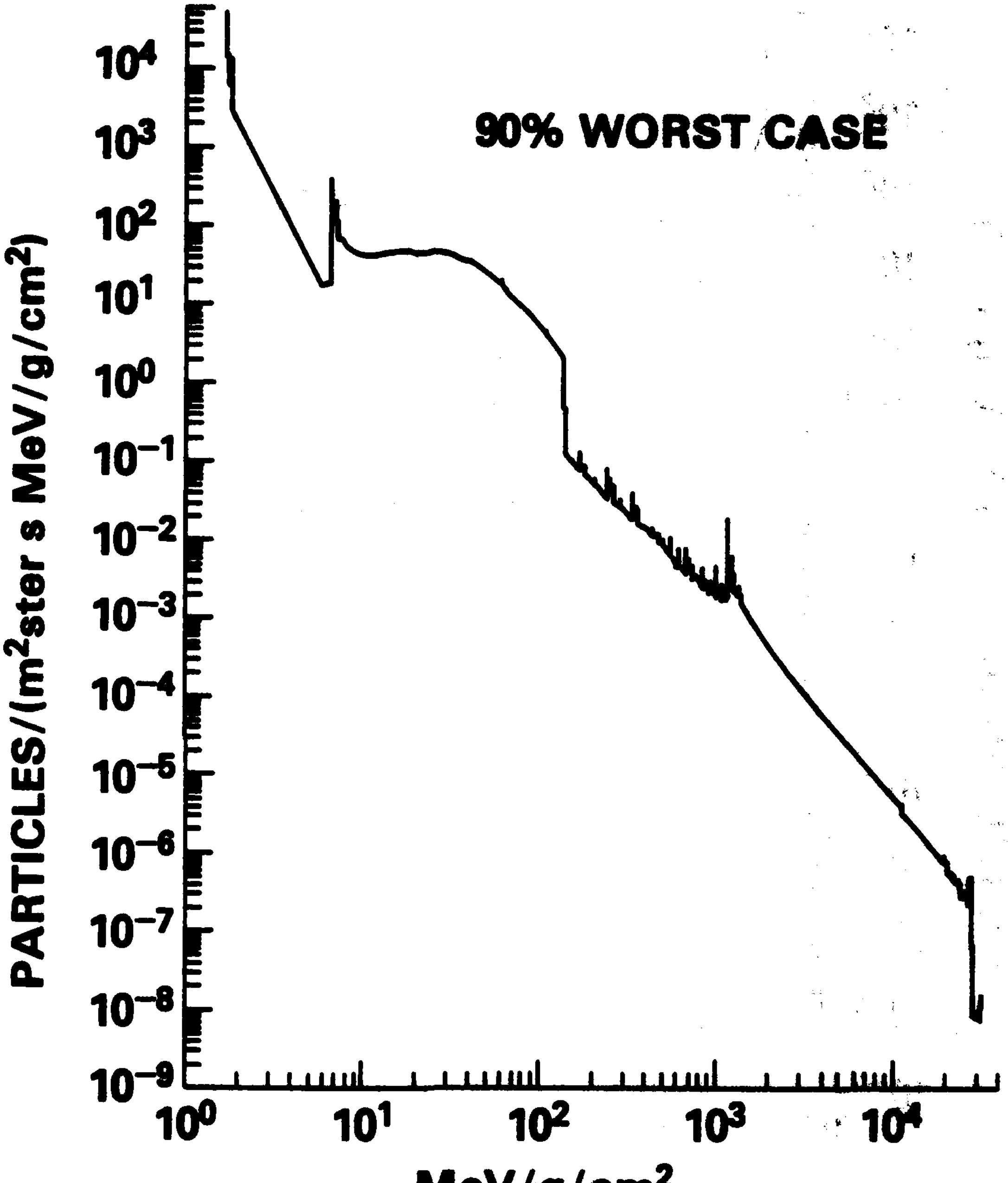

Figure 3. 90 percent worst case spectrum. LET spectrum due to galactic cosmic rays at times of minimum solar activity plus 90 percent worst case contribution of low energy particles due to solar and interplanetary activity.

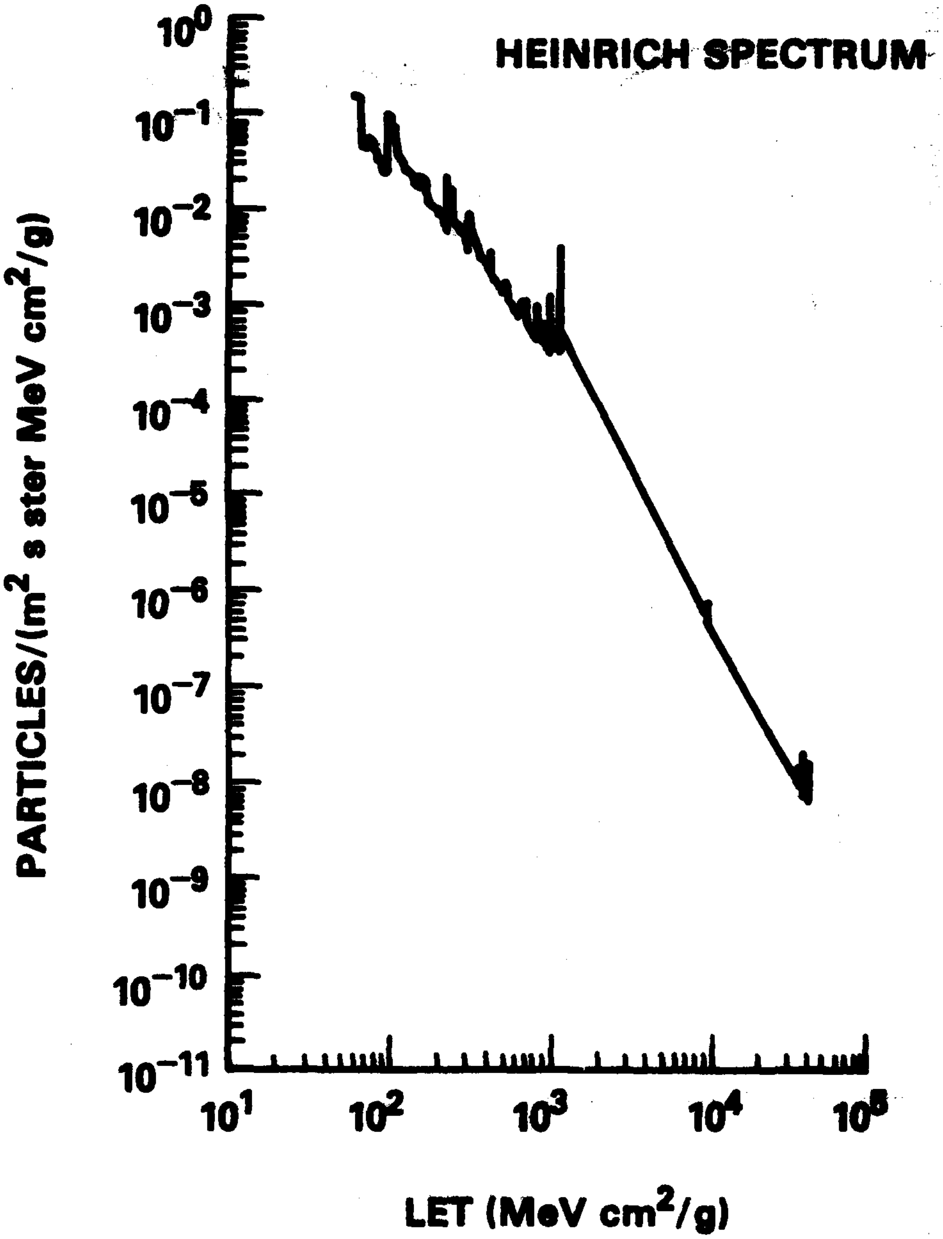

Figure 4. Cosmic-ray LET spectrum behind 0 g/cm^2 shielding due to Heinrich.

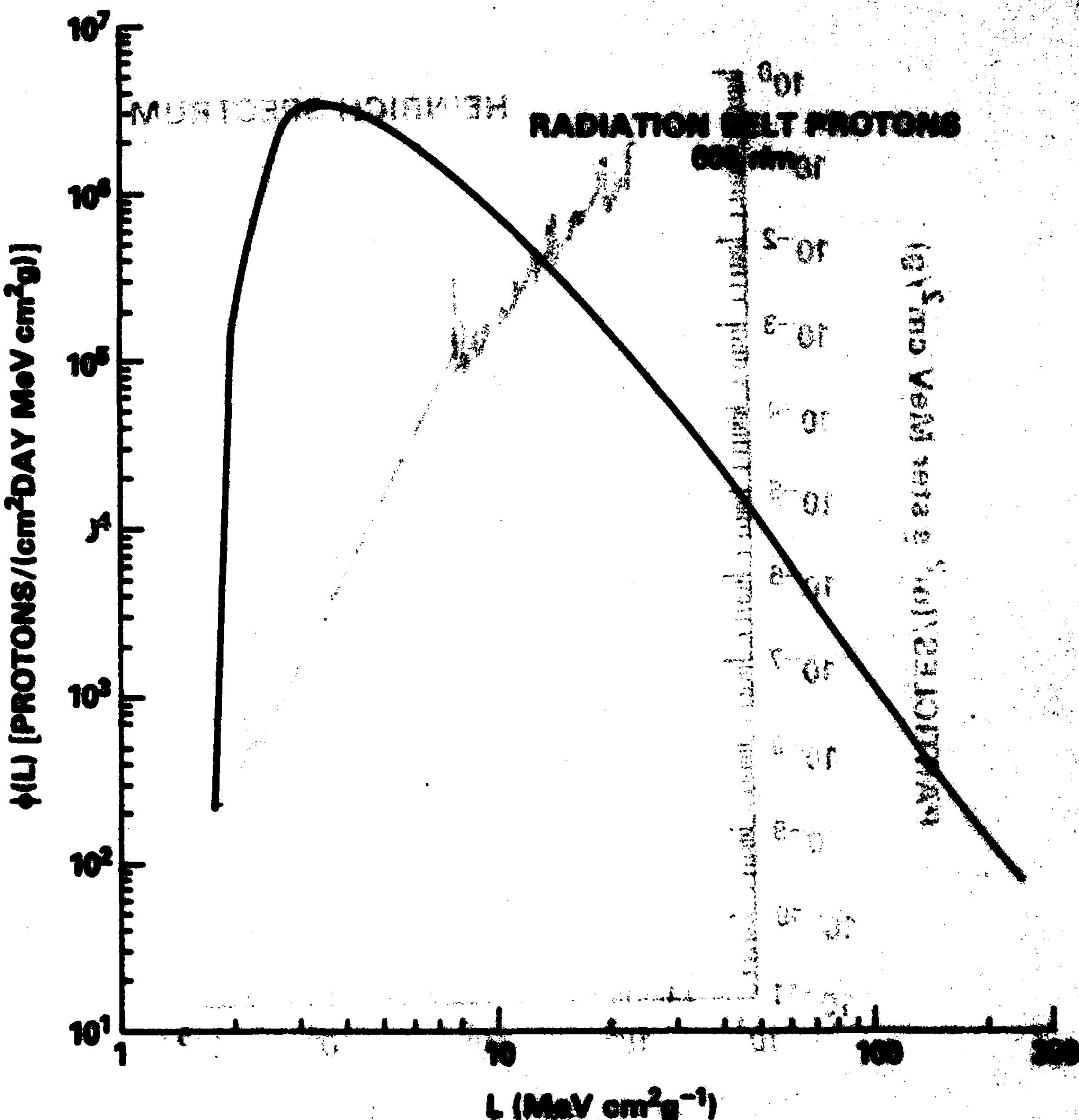

Figure 5. LET spectrum for protons for a 600 nautical mile orbit in the proton radiation belts.

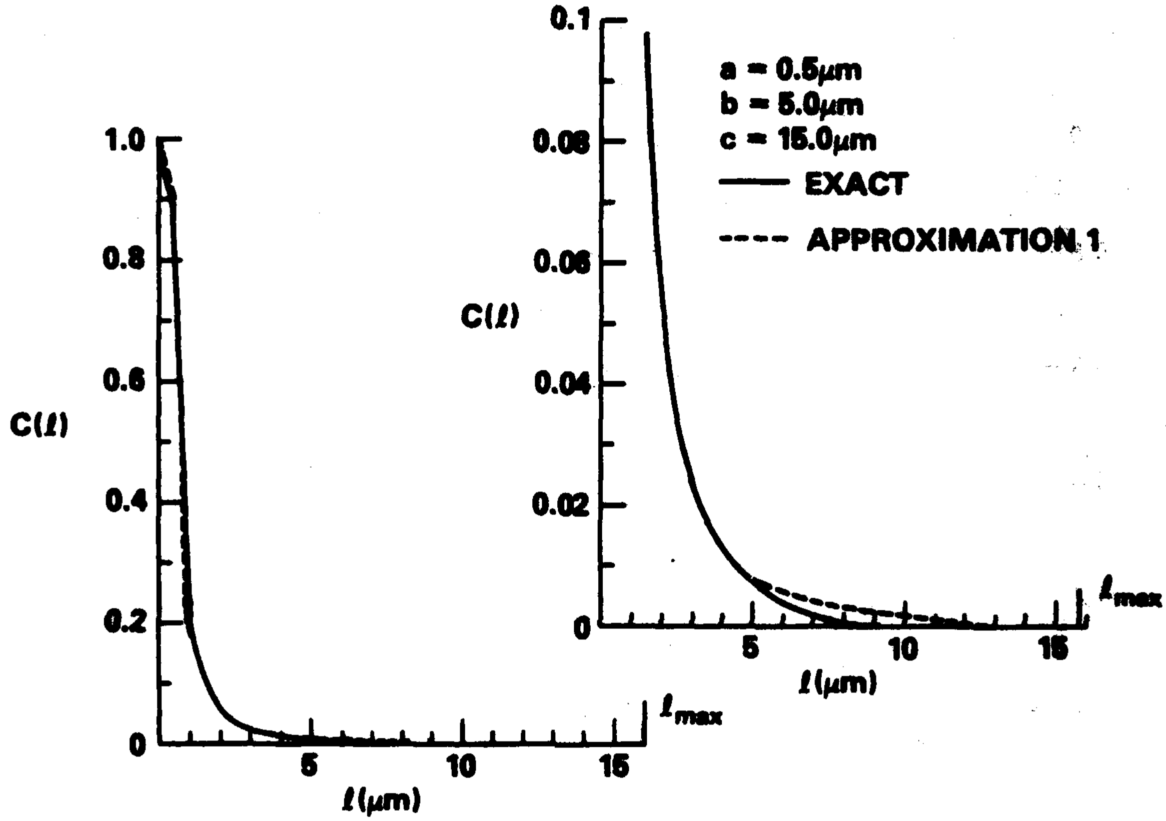

Figure 6. Integral chord-length distribution for 0.5 x 5 x 15 micrometer parallelepiped. Comparison of exact evaluation and Approximation 1.

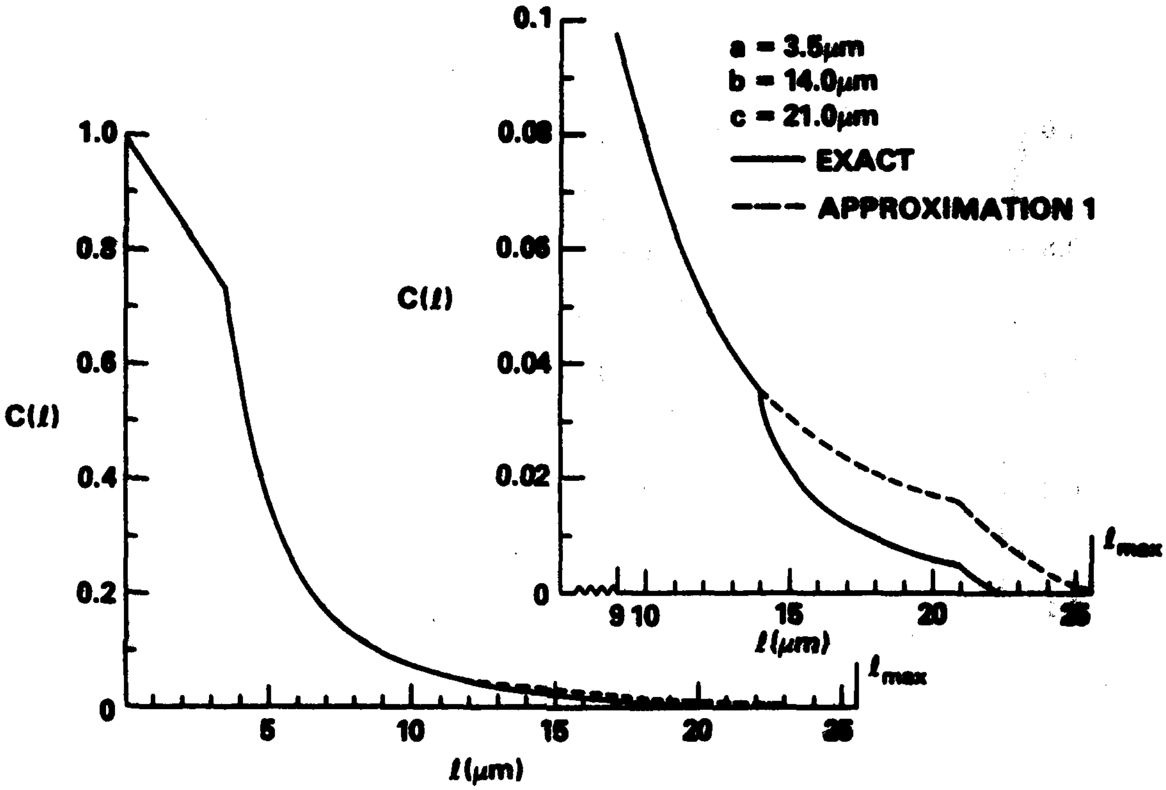

Figure 7. Integral chord-length distribution for 3.5 x 14 x 21 micrometer parallelepiped. Comparison of exact evaluation and Approximation 1.

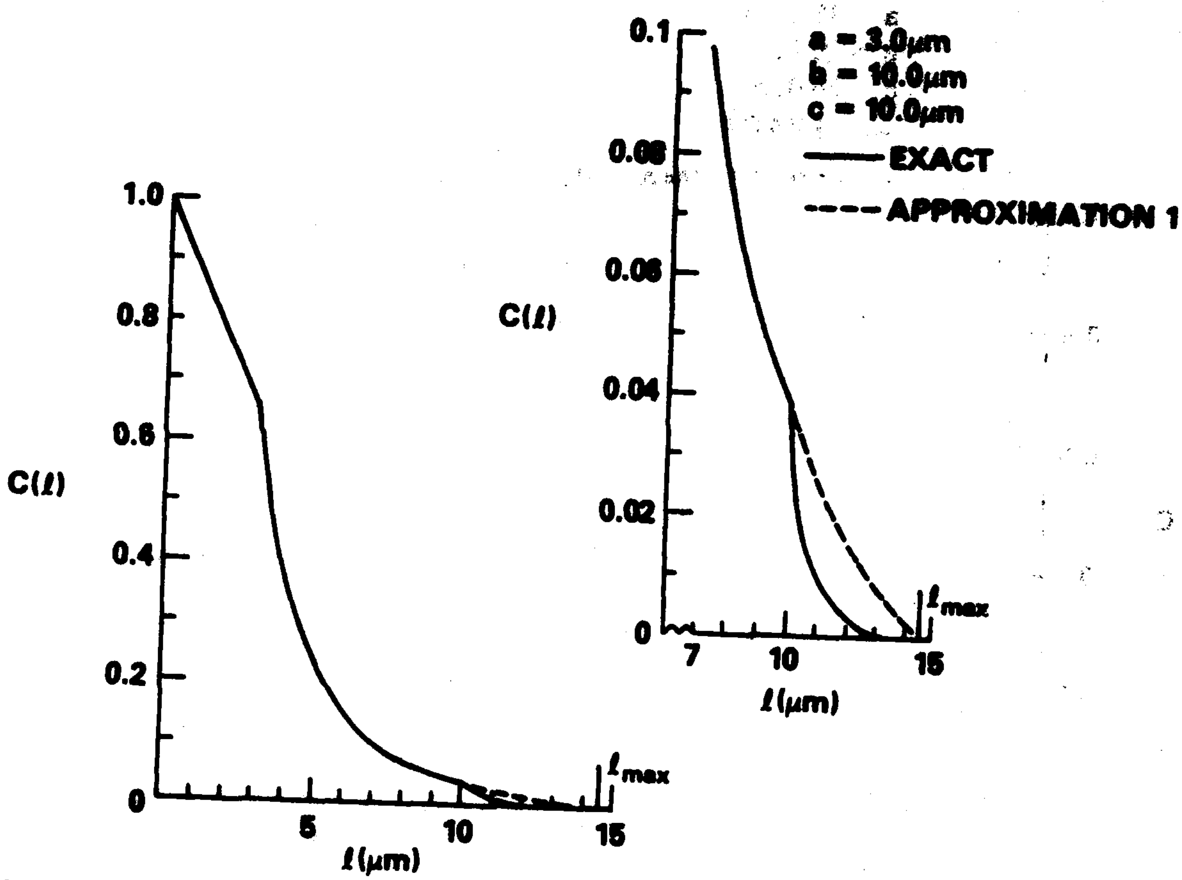

Figure 8. Integral chord-length distribution for 3 x 10 x 10 micrometer parallelepiped. Comparison of exact evaluation and Approximation 1.

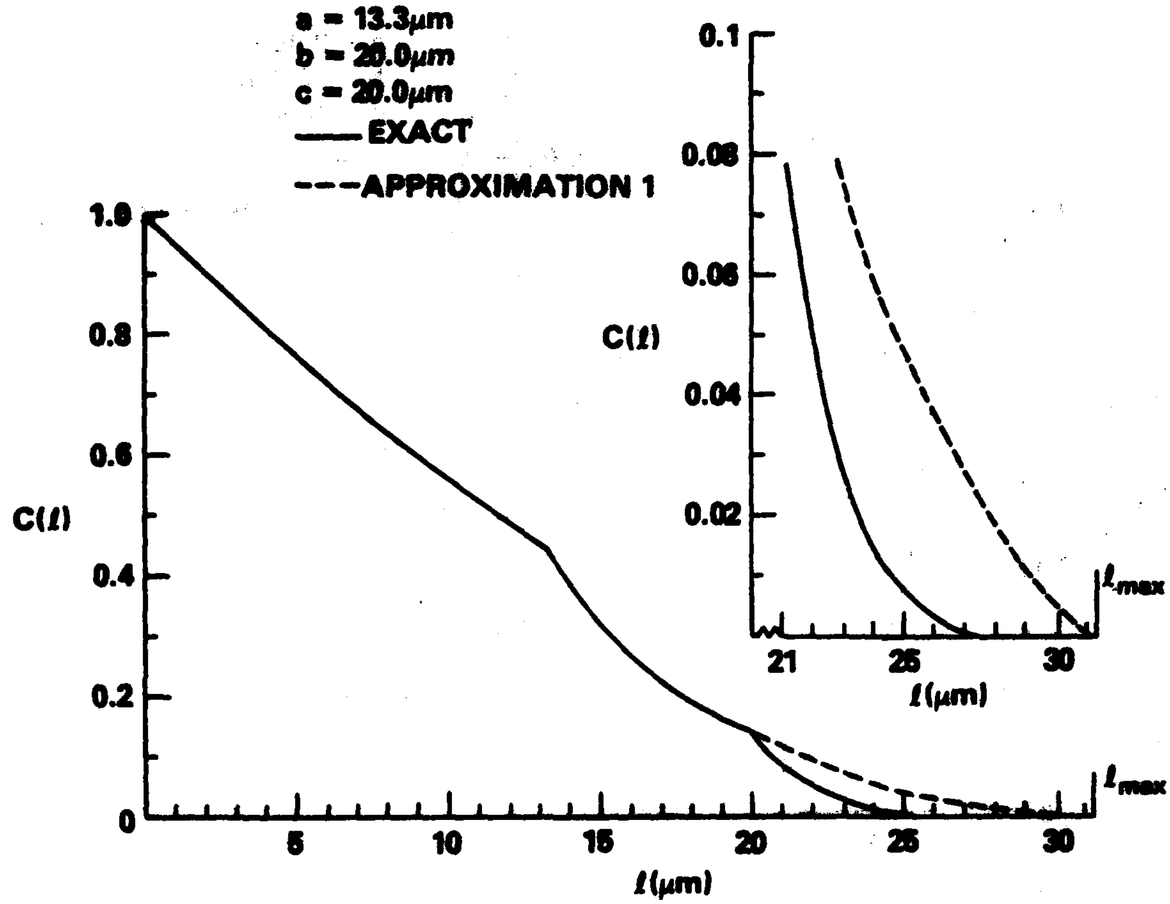

Figure 9. Integral chord-length distribution for 13.3 x 20 x 20 micrometer parallelepiped. Comparison of exact evaluation and Approximation 1.

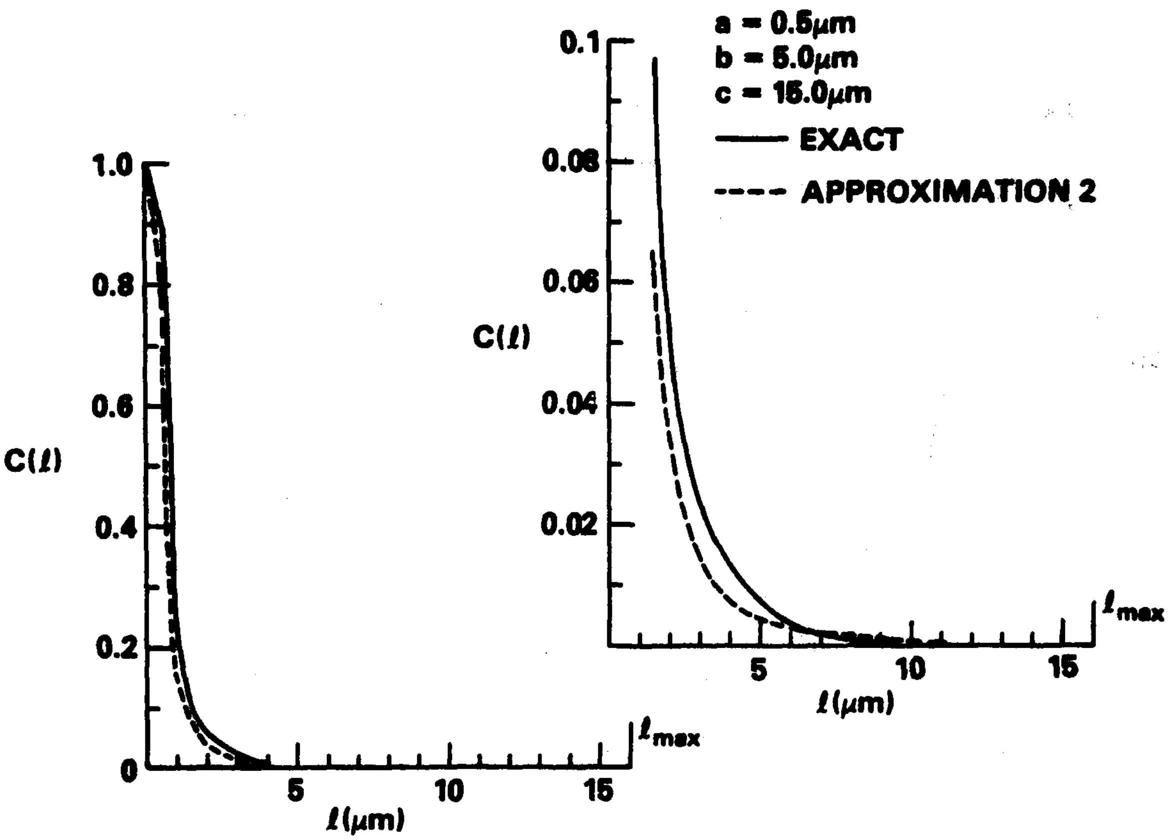

Figure 10. Integral chord-length distribution for 0.5 x 5 x 15 micrometer parallelepiped. Comparison of exact evaluation and Approximation 2.

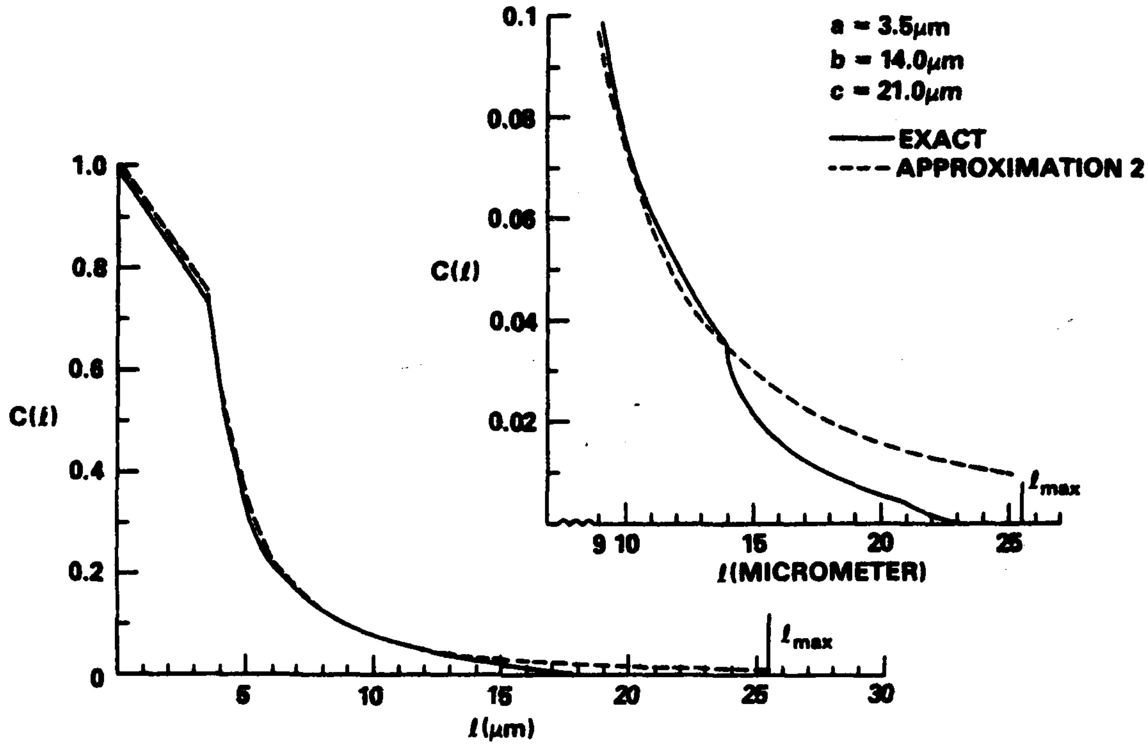

Figure 11. Integral chord-length distribution for 3.5 x 14 x 21 micrometer parallelepiped. Comparison of exact evaluation and Approximation 2.

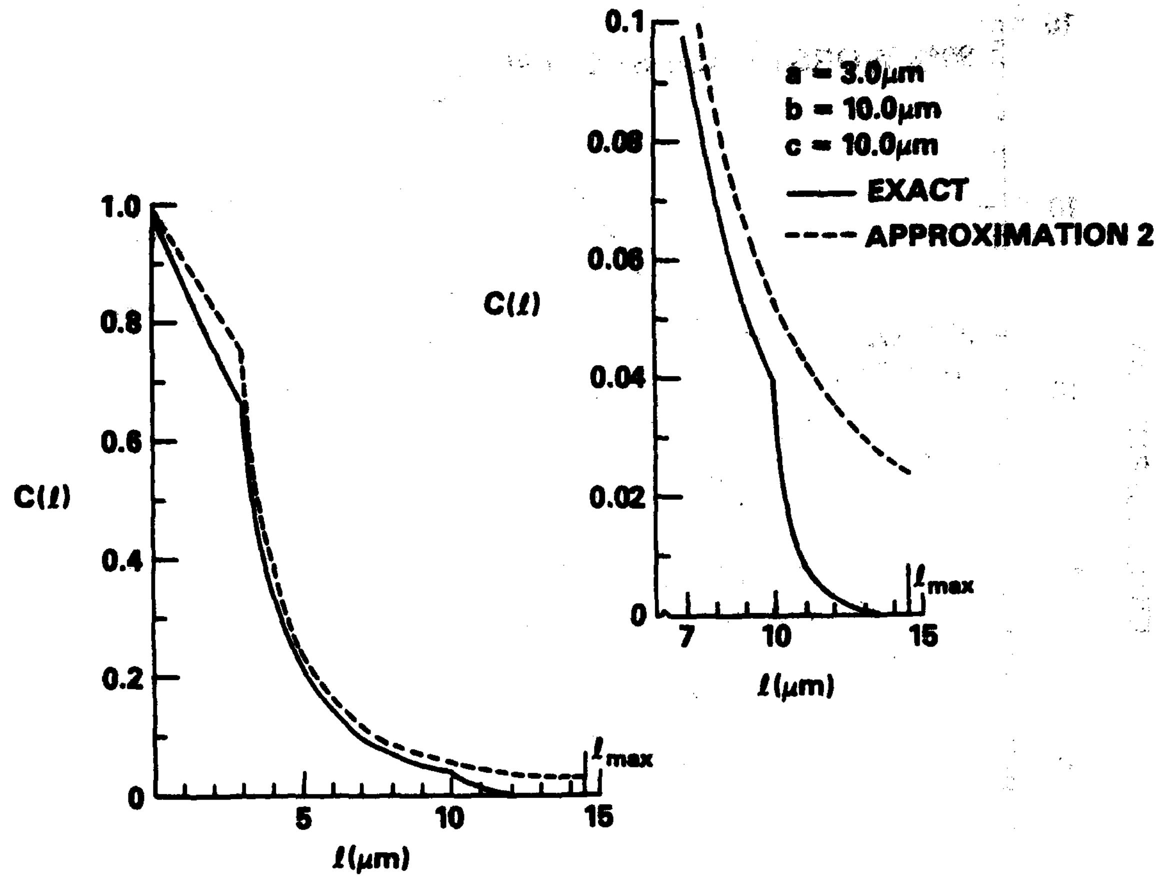

Figure 12. Integral chord-length distribution for 3 x 10 x 10 micrometer parallelepiped. Comparison of exact evaluation and Approximation 2.

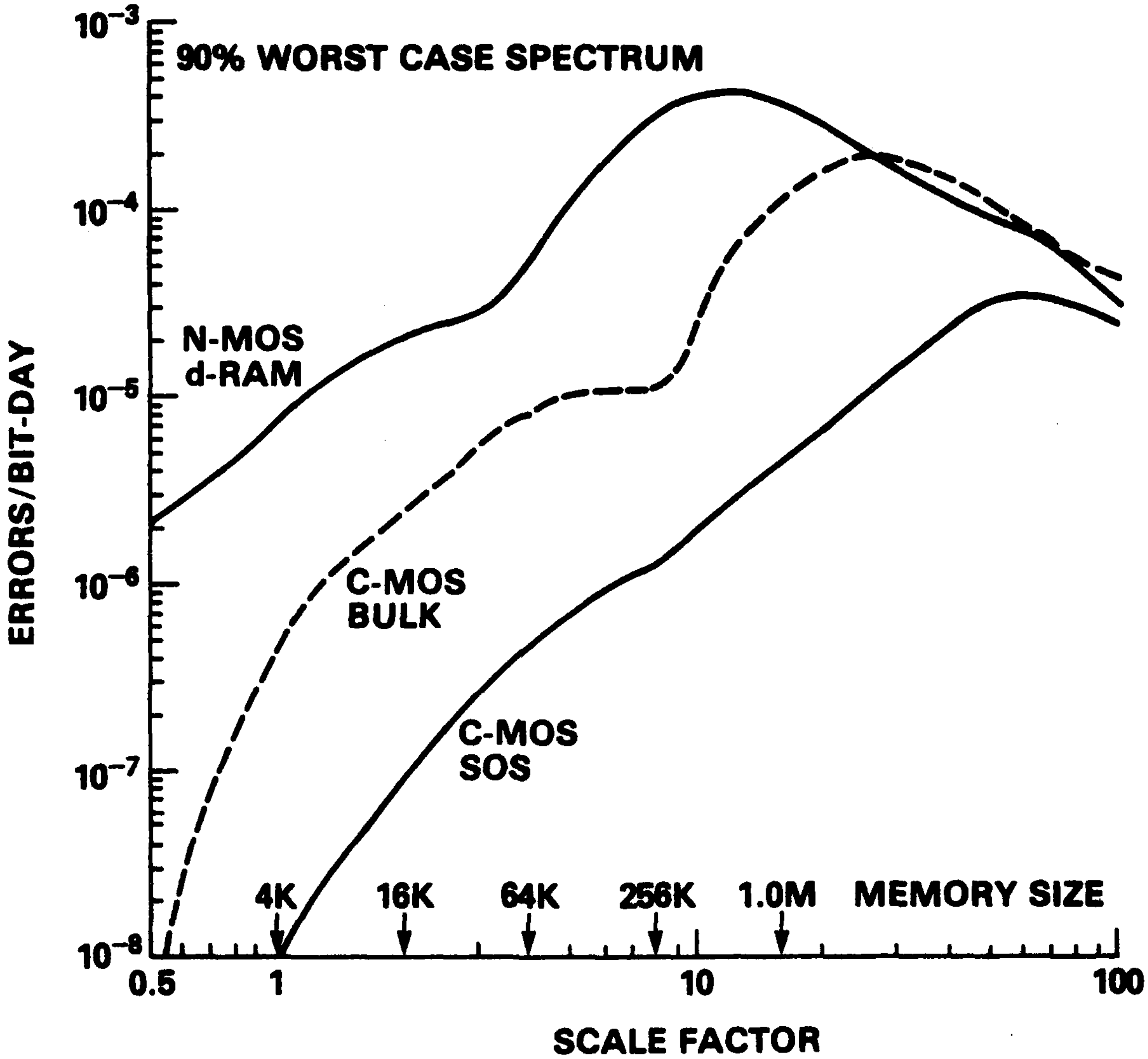

Figure 13. Comparison of scaling of soft-upset rate for three device types in the 90 percent worst case spectrum environment for ΔE varying as α^{-3}.

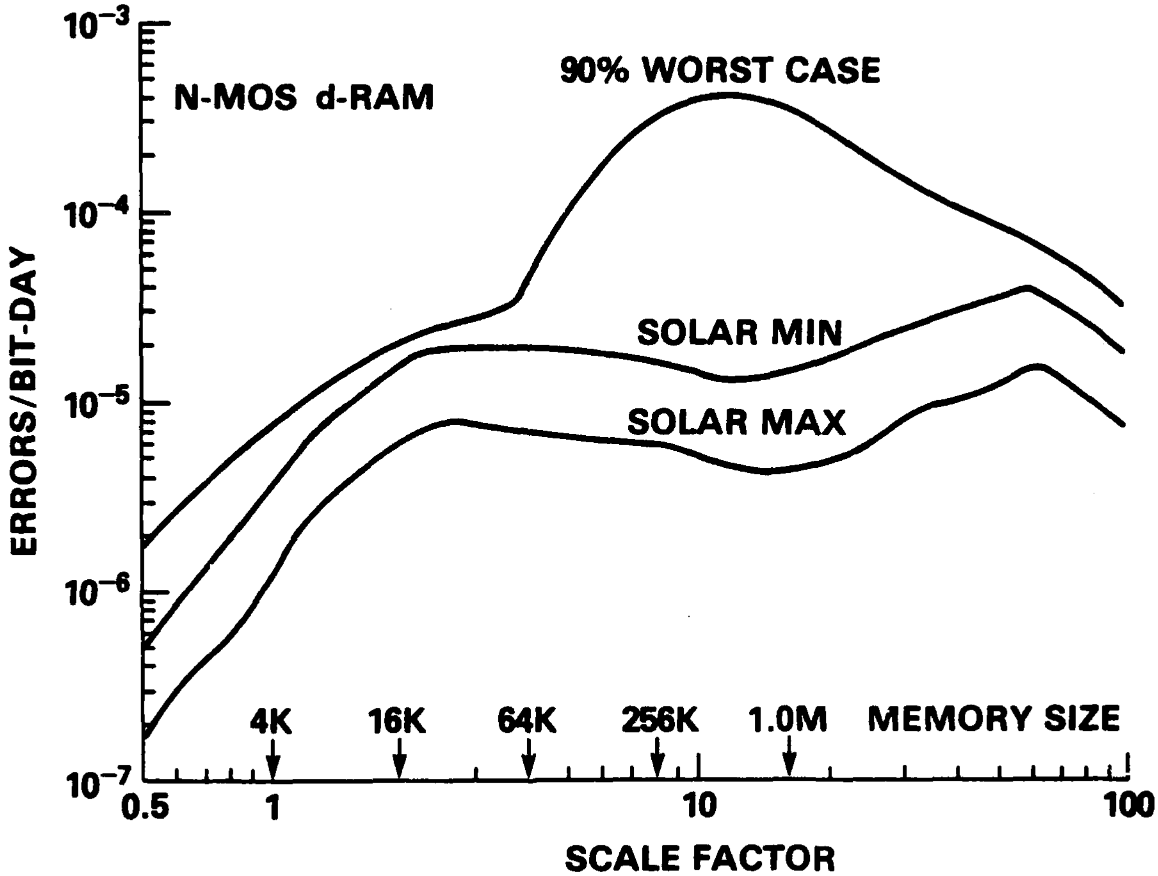

Figure 14. Prediction of soft-upset rate for N-MOS dynamic RAM in three different cosmic ray environments for ΔE varying as α^{-3}.

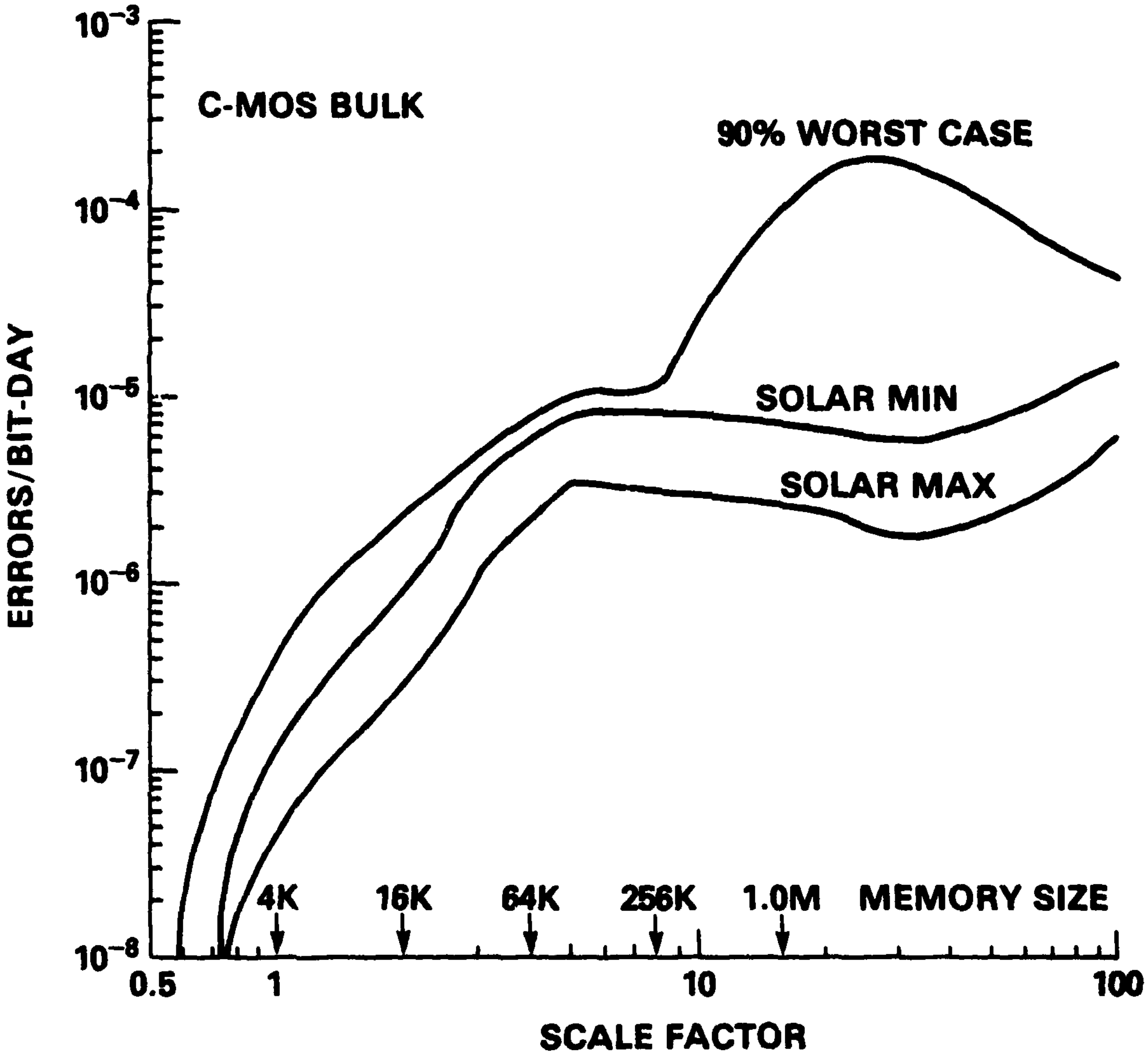

Figure 15. Prediction of soft-upset rate for CMOS bulk static RAM in three different cosmic ray environments for ΔE varying as α^{-3}.

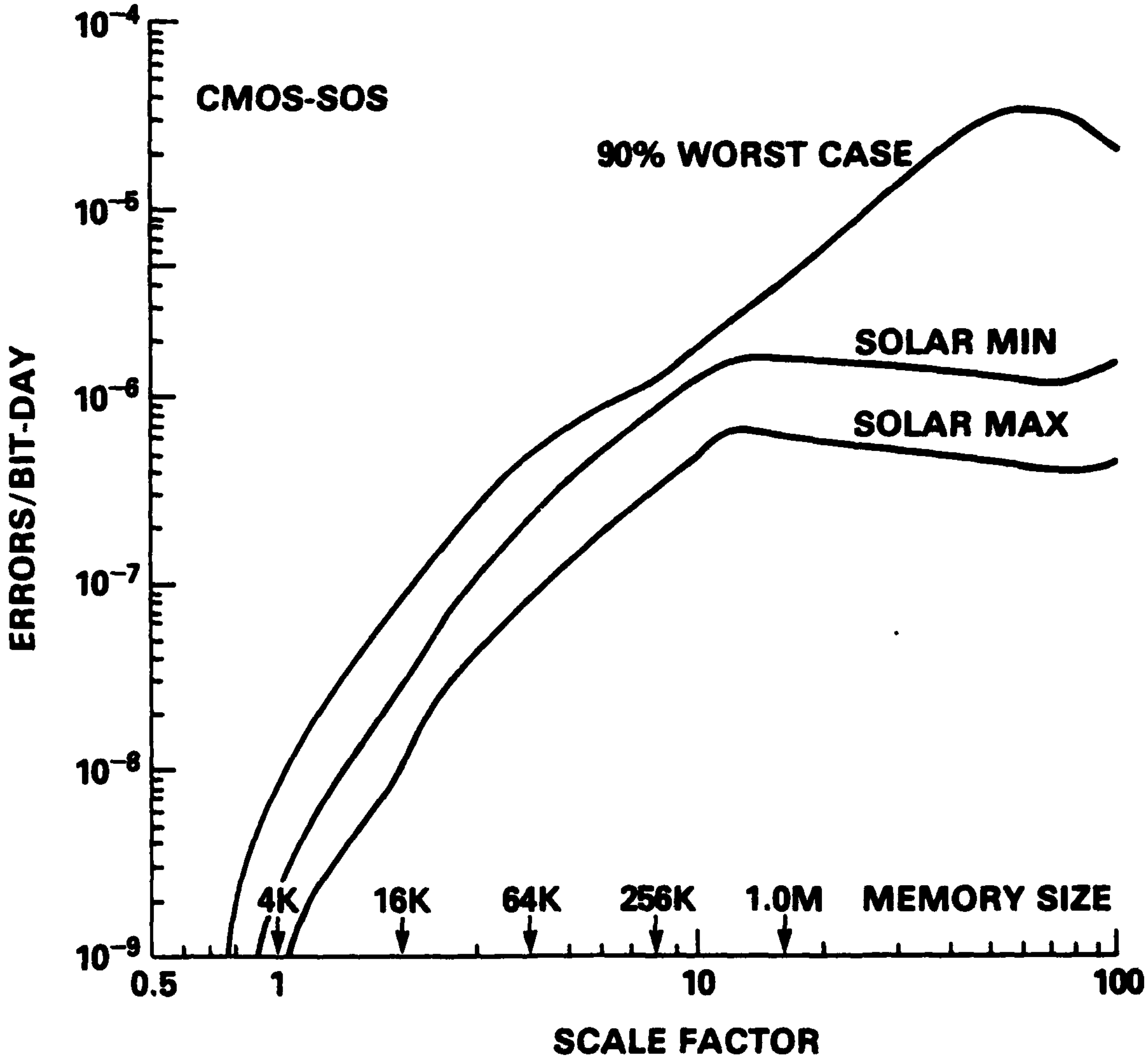

Figure 16. Prediction of soft-upset rate for CMOS-SOS static RAM in three different cosmic ray environments for ΔE varying as α^{-3}.

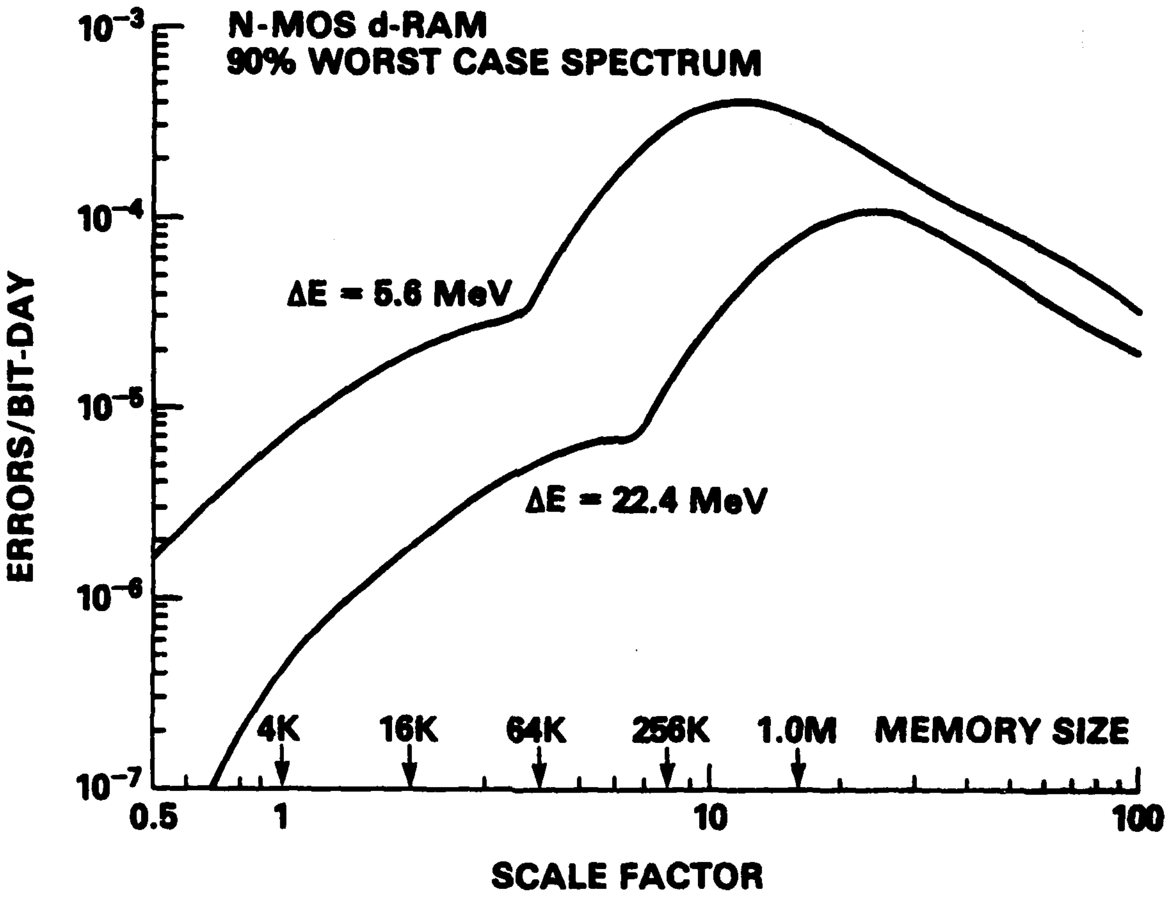

Figure 17. Effect of change in critical energy, ΔE, on predicted soft-upset vulnerability of N-MOS d-RAM in 90 percent worst case spectrum environment. Scaling assumed ΔE varies as α^{-3}.

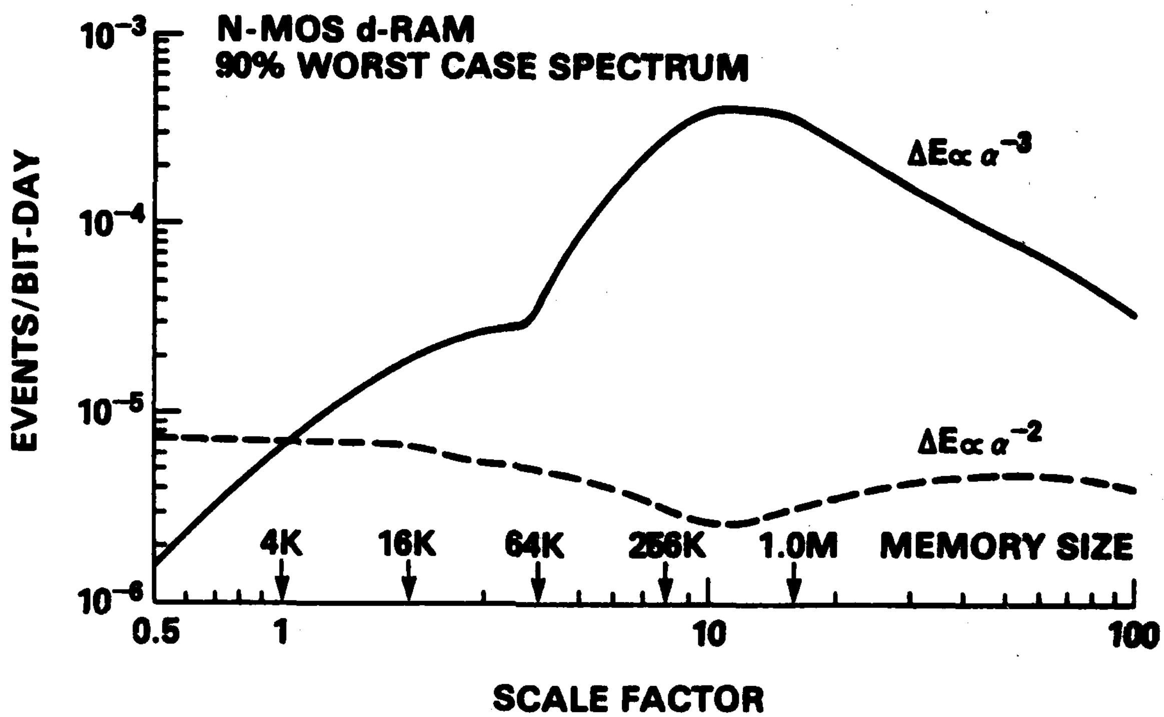

Figure 18. Effect of scaling scenario, ΔE varying as α^{-3} vs ΔE varying as α^{-2}, on predicted soft-upset rate for N-MOS dynamic RAM.

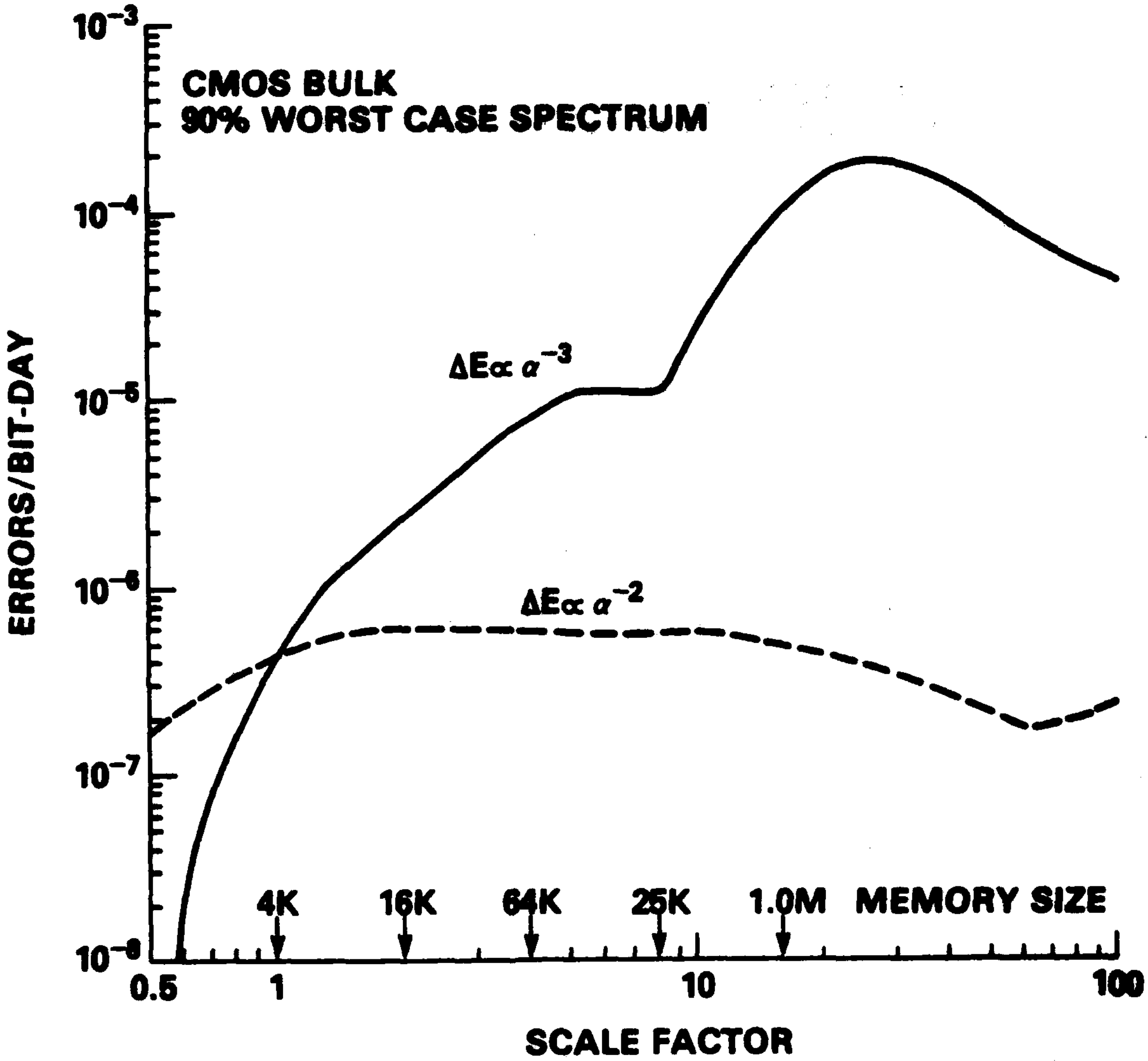

Figure 19. Effect of scaling scenario, ΔE varying as α^{-3} vs ΔE varying as α^{-2}, on predicted soft-upset rate for CMOS bulk static RAM.

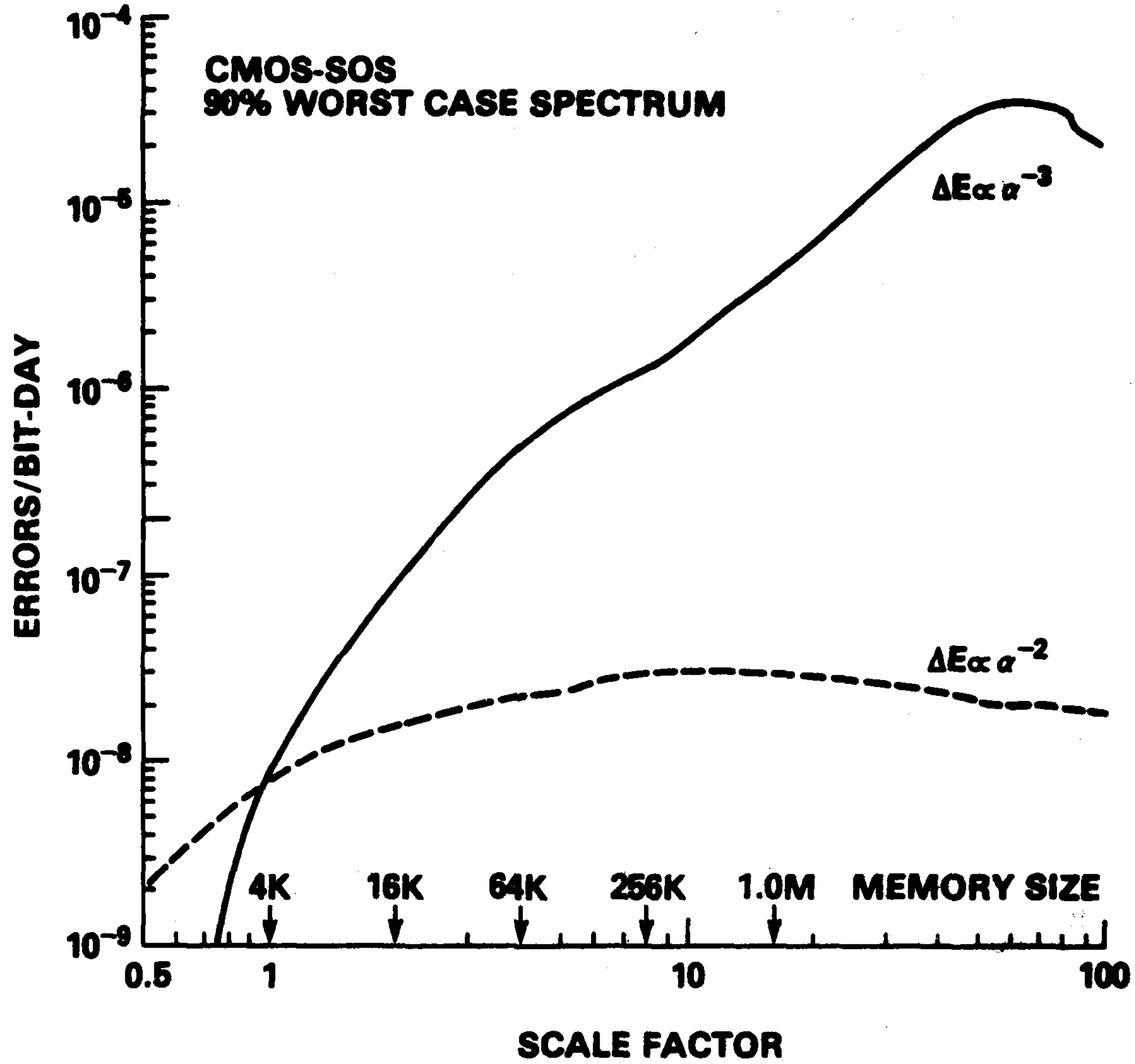

Figure 20. Effect of scaling scenario, ΔE varying as α^{-3} vs ΔE varying as α^{-2}, on predicted soft-upset rate for CMOS-SOS static RAM.

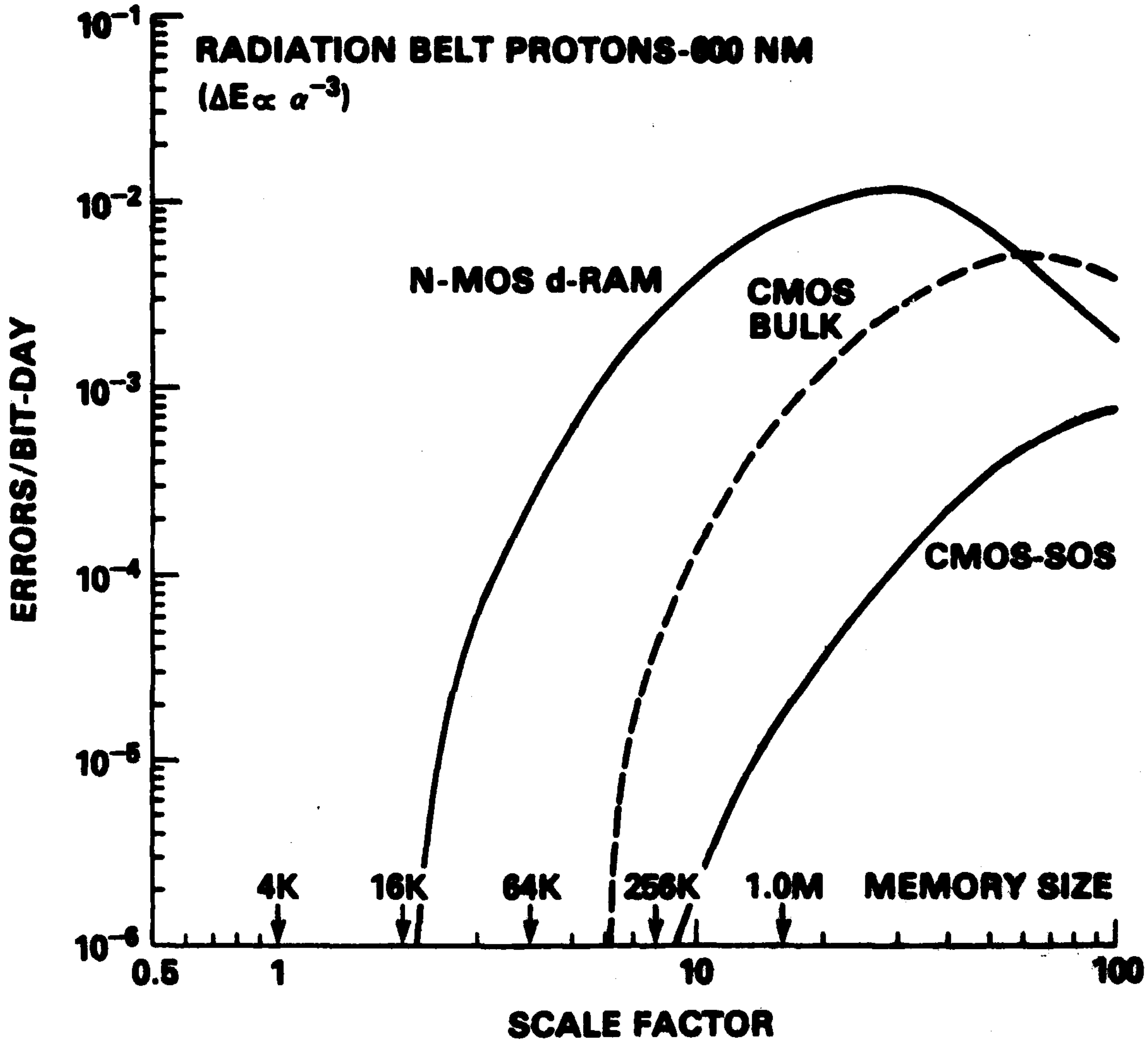

Figure 21. Prediction of soft upset rate due to direct ionization by radiation belt protons at 600 nautical miles for critical energy scaling as α^{-3}.

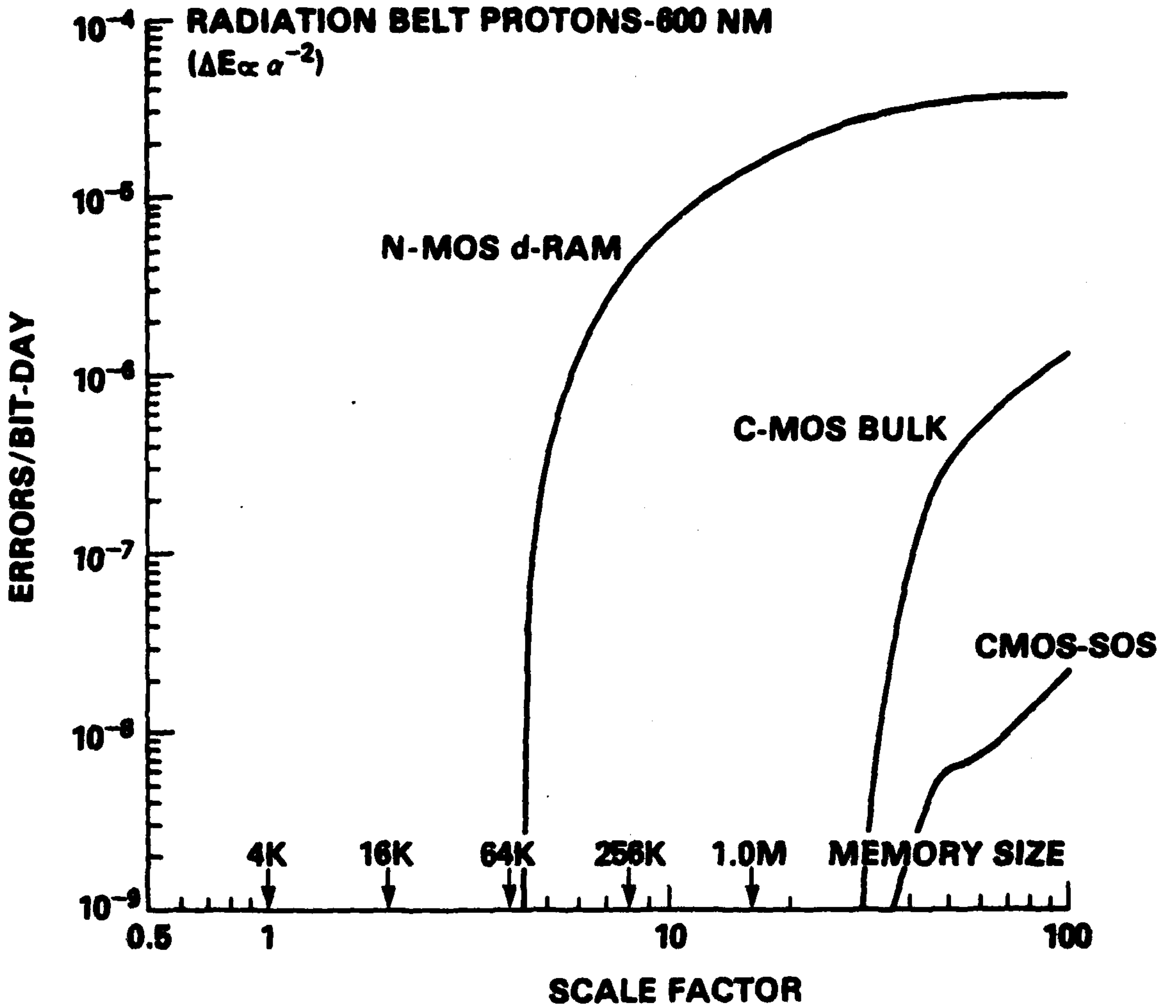

Figure 22. Prediction of soft upset rate due to direct ionization by radiation belt protons at 600 nautical miles for critical energy scaling as α^{-2}.

TABLE I. Parameters Used in Soft-Upset Calculations

Device Type	Device Dimensions for 4k Reference Device (Scale Factor = 1) (μm)	Critical Energy (MeV)	Error Conversion Factor
N-MOS d-RAM	3.5 x 14 x 21	5.6	0.5
N-MOS d-RAM	3.5 x 14 x 21	22.5	0.5
CMOS-Bulk Static RAM	3 x 10 x 10	22.5	3.0
CMOS-SOS Static RAM	0.5 x 5 x 15	24.75	5.0

REFERENCES

1. J. F. Ziegler and W. A. Lanford, Science 206, 776 (1979). Effect of Cosmic Rays on Computer Memories.

2. Edward A. Burke, RADC-TM-81-ES-03 (16 June 1979), Rome Air Development Center. The Effect of Size Reduction on Cosmic Ray Induced Errors in RAMs.

3. J. H. Adams, Jr., R. Silberberg, and C. H. Tsao, NRL Memorandum Report 4506 (August 25, 1981). Cosmic Ray Effects on Microelectronics, Part I: The Near-Earth Particle Environment.

4. W. Heinrich, Radiation Effects 34, 143 (1977). Calculation of LET-Spectra of Heavy Cosmic Ray Nuclei at Various Absorber Depths.

5. E. Petersen, IEEE Trans. Nucl. Sci., NS-28, 3981 (1981). Soft Errors Due to Protons in the Radiation Belt.

6. D. M. Sawyer and J. I. Vette, NSSDC/WDC-A-R&S 76-06 (December 1976). AP-8 Trapped Proton Environment for Solar Maximum and Solar Minimum.

7. C. Williamson and J. P. Boujot, CEA Report No. 2189 (1962). Tables of Range and Rate of Energy Loss of Charged Particles of Energy, 0.5 to 150 MeV.

8. E. L. Petersen, IEEE Trans. Nucl. Sci., NS-27, 1494 (1980). Nuclear Reactions in Semiconductors.

9. John N. Bradford, J. Appl. Phys. 50, 3799 (1979). A distribution function for ion track lengths in rectangular volumes.

10. C. M. Hsieh, P. C. Murley, and R. R. O'Brien, IEEE Electron Dev. Ltrs. EDL-2, 103 (1981). A Field-Funneling Effect on the Collection of Alpha-Particle-Generated Carriers in Silicon Devices.

11. A. B. Campbell and A. R. Knudson, Charge Collection Measurements for Energetic Ions in Silicon, to be presented at 19th Annual Conference on Nuclear and Space Radiation Effects, July 20-22, 1982.

12. Albrecht M. Kellerer, Rad. Res. 47, 359 (1971). Considerations on the Random Traversal of Convex Bodies and Solutions for General Cylinders.

13. J. C. Pickel and J. T. Blandford, IEEE Trans. Nucl. Sci. NS-27, 1006 (1980). Cosmic-Ray-Induced Errors in MOS Devices.

14. R. Coleman, J. Appl. Prob. 6, 430 (1969). Random Paths Through Convex Bodies.

15. John N. Bradford, Space Systems and Their Interactions with Earth's Space Environment. Progress in Astronautics and Aeronautics 71, 349 (1980). Cosmic Ray Effects in Very Large Scale Integration.

16. J. F. Ziegler and W. A. Lanford, J. Appl. Phys. 52, 4305 (1981). The effect of sea level cosmic rays on electronic devices.

17. Carver Mead and Lynn Conway, "Introduction to VLSI Systems," Addison-Wesley Publishing Co., Reading, MA, 1980, p. 33.

18. J. C. Pickel and J. T. Blandford, Jr., IEEE Trans. Nucl. Sci. 25, 1166 (1978). Cosmic Ray Induced Errors in MOS Memory Cells.

DISTRIBUTION LIST

External

Dr. Lorenzo J. Abella
Office of the Deputy Asst Secretary
of the Navy (RAST)
Pentagon 5E731
Washington, DC 20350

Dr. Mario H. Acuna
NASA
Goddard Space Flight Center
Code 695
Greenbelt, MD 20771

Dr. Orville Adams
TRW Incorporated
Defense & Spa. Sys. Group
One Space Park
Redondo Beach, CA 90278

Mr. John W. Adophsen
NASA, GSFC
Code 311A
Greenbelt, MD 20771

Mr. David Alexander
Mission Research Corporation
1400 San Mateo Blvd SE
Suite A
Albuquerque, NM 87108

Mr. William Alfonte
KAMAN-Tempo
2560 Huntington Avenue
Suite 300
Alexandria, VA 22303

Mr. John Andrews
General Electric Co.
P.O. Box 8555
Philadelphia, PA 19101

Mr. Robert Antinone
BDM Corporation
1801 Randolph Rd, SE
Albuquerque, NM 87106

Dr. Itsu Arimura
Boeing Corp.
MS 2R-00 P.O. Box 3999
Seattle, WA 98124

Mr. Robert Armistead
ARACOR
1223 E. Arques Avenue
Sunnyvale, CA 94086

Dr. Joseph Azarewicz
JAYCOR
11011 Torreyana Road
San Diego, CA 92138

Dr. Ali Bahraman
Northrop
1 Research Park
Palos Verdes, CA 90274

Dr. Ben Bernstein
NASA Headquarters
Office of the Chief Engineer
Code DP
Washington, DC 20546

Mr. Bernard Blake
The Aerospace Corp.
P.O. Box 92957
Los Angeles, CA 90009

Mr. James Blandford
Rockwell International
Science Center
3370 Miroloma
Anaheim, CA 93802

Mr. Stewart Bower
Aerospace Cirporation
P.O. Box 92957
Los Angeles, CA 90009

Dr. John N. Bradford
RADC/ESR
Dept for Electronic Tech.
M/S 64
Hanscom AFB, MA 01731

Mr. George J. Brucker
RCA Laboratory
Princeton, NJ 08540

Dr. R. Buchanan
ATTN: ESR
Rome Air Development Center
Hanscom AFB, MA 01731

Dr. Paltiel Buckman
Aerospace Corporation
2350 E. El Segundo Blvd
El Segundo, CA 90009

Dr. Edward A. Burke
RADC ESR/ET
M/S 64
Hanscom AFB, MA 01731

Dr. Alan Carlan
The Aerospace Corp.
P.O. Box 92957
Los Angeles, CA 90009

Dr. Larry R. Cooper
Code 427
Office of Naval Research
800 N. Quincy Street
Arlington, VA 22217

Mr. Floyd Coppage
Sandia Laboratories
P.O. Box 5800, D/4365
Albuquerque, NM 87111

Mr. W.W.W. T. Crane
A2/1083
Aerospace Corp.
P.O. Box 92957
Los Angeles, CA 90009

Maj. John Criscuolo
Space Division/YLX
P.O. Box 92960
Los Angeles, CA 90009

Mr. Vitaly Danchenko
Code 654.2
NASA-GSFC
Greenbelt, MD 20771

Dr. Edward S. Davidson
Illinois Computer Research Inc.
1217 Foothill Dr.
Champaign, Il 61820

Mr. William Dawes
Sandia Laboratories
Division 2144
Albuquerque, Nm 87185

Dr. Harvey Eisen
DELHD-NRBH
Harry Diamond Laboratory
2800 Powder Mill Rd.
Adelphi, MD 20783

Mr. Thomas Ellis
Naval Weapons Support Center
Code 3073, Bldg. 2917
Crane, IN 47522

Mr. James Ferry
Air Force Weapons Laboratory (NTYC)
Kirtland AFB, NM 92402

Mr. Robert Filz
AFGL-PLIG
Hanscom AFB, MA 01731

Dr. Roger Fitzwilson
Science Applications, Inc.
1200 Prospect Street
La Jolla, CA 92038

Mr. Thomas Frey
Control Data Corporation
2300 E. 88th St.
Bloomington, MN 55420

Dr. Arthur Friedman
George Washington Univ.
School of Eng. & Applied Sciences
Washington, DC 20052

Dr. K.F. Galloway
National Bureau of Standards
Technology Bldg., Rm A-305
Washington, DC 20234

Mr. George Gilley
The Aerospace Corp.
P.O. Box 92957
Los Angeles, CA 90009

Mr. Dennis Grimes
Westinghouse Electric
Radiation Effects Technology
P.O. Box 1521 M/S 3330
Baltimore, MD 21203

Dr. Harold L. Grubin
Scientific Research Associates
P.O. Box 498
Gastonbury, CN 06033

Mr. Leon Hamiter
NASA Marshall Space Flight Center
Code EC43
Huntsville, AL 35812

Mr. John Harrity
IRT Corporation
P.O. Box 80817
San Diego, CA 92138

Dr. David Haykin, Jr.
Code 710.2, Bldg 22
NASA, GSFC
Greenbelt, MD 20771

Maj. Burl Hickman
Defense Nuclear Agency (RAEV)
6801 Telegraph Road
Alexandria, VA 20305

Lt. Col. Steven Hunter
Space Division
Air Force Systems Comd.
P.O. Box 92960
Worldway Postal Center
Los Angeles, CA 90009

Mr. Alan Johnston
Boeing Aerospace Company
MS-2R-00
P.O. Box 3999
Seattle, WA 98124

Mr. Vern Josephson
The Aerospace Corp.
P.O. Box 93957
Los Angeles, CA 90009

Mr. Roger Judge
IRT Corp.
7650 Convoy Ct.
P.O. Box 80817
San Diego, CA 92138

Dr. Frank Junga
Lockheed Research Lab.
3251 Hanover St.
52/54-202
Palo Alto, CA 92304

Maj. Daniel D. Kadel
Defense Nuclear Agency
RAEV
Washington, DC 20305

Mr. Henry Kalapaca
Westinghouse Electric Corporation
Radiation Effects Technology
P.O. Box 1521 M/S 3330
Baltimore, MD 21203

Mr. Robert Karpen
Code DP
NASA Headquarters
Washington, DC 20546

Capt. Craig Kimberlin
Defense Nuclear Agency
RAEV
6801 Telegraph Road
Alexandria, VA 20305

Mr. Everett King
Northrup Electronics Div.
2301 W. 120th Street (C 3323/WC)
Hawthorne, CA 90250

Mr. Jack Kinn
Electronic Industries Assoc.
2001 Eye Street, NW
Washington, DC 20006

Mr. Robert Kloster
McDonnell Douglas Corp.
Dept. E451
P.O. Box 526
St. Louis, MO 62166

Dr. W. A. Kolasinski
P.O. Box 92957
Aerospace Corp.
Los Angeles, CA 90009

Mr. Clyde Lane
Rome Air Development Center
RADC/RBRP
Griffiss AFB, NY 13441

Mr. David Long
Science Applications Inc.
1200 Prospect Street
La Jolla, CA 92038

Dr. Thomas T. Marquitz
Central Intelligence Agency
Washington, DC 20505

Dr. Gerald Masson
Dept. of Elec. Engin.
Barton Hall
Johns Hopkins University
Baltimore, MD 21218

Mr. Timothy May
Intel Corp.
Mail Stop WW2-265
3885 S.W. 198th Ave.
Aloha, OR 97077

Mr. Sheldon Meth
The BDM Corp.
7915 Jones Branch Dr.
McLean, VA 22102

Dr. James McGarrity
DELHD-NW-RC
Harry Diamond Laboratory
2800 Powder Mill Rd.
Adelphi, MD 20783

Prof. T.C. McGill
California Inst. of Tech.
Pasadena, CA 91125

Mr. William E. McInnis
Code D
Office of the Chief Engineer
NASA
Washington, DC 20546

Dr. Peter J. McNulty
Clarkson College of Technology
Potsdam, NY 13676

Mr. R.J. McPartland
Bell Labs.
555 Union Blvd.
Allentown, PA 18103

Dr. John Meason
ATTN: STEWS-TE-AN
White Sands Missile Range
White Sands Missile Range, NM
88002

Mr. George Messenger
3111 Bel Air Drive, 7-F
Las Vegas, NV 89109

Mr. Douglas Millward
Science Applications, Inc.
1200 Prospect St., MS #1
La Jolla, CA 92038

Mr. E Gary Mullen
AFGL-PHG, M/S 30
Hanscom AFB, MA 01731

Mr. John Mullis
ATTN: ELP
Air Force Weapons Laboratory
Kirtland AFB, NM 87117

Ms. Deb Newbury
Control Data Corp.
BRR 142
2300 E. 88th Street
Bloomington, MN 35420

Mr. Donald Nichols
Jet Propulsion Lab
T-1180
4800 Oak Grove Drive
Pasadena, CA 91003

Dr. Wm. Oldham
Electrical Engineering Dept.
University of California
Berkley, CA 94720

Dr. Les Palkuti
ARACOR
1223 E. Argues Avenue
Sunnyvale, CA 94086

Dr. Joseph Peden
General Electric Co.
Valley Forge Space Center
P.O. Box 8555
Philadelphia, PA 19101

Mr. Howard Phillips
Electronics Research Laboratory
The Aerospace Corporation
P.O. Box 92957
Los Angeles, CA 90009

Mr. James C. Pickel
Rockwell International
3370 Miraloma Ave,
Code 031-BB01
Anaheim, CA 92803

Mr. William E. Price
Jet Propul Lab., T-1180
Cal. Inst. Tech.
4800 Oak Grove Drive
Pasadena, CA 91003

Mr. James Ramsey
Naval Weapons Support Center
Code 7024
Crane, IN 47522

Mr. James Raymond
Mission Research Corp.
P.O. Box 1209
La Jolla, CA 92038

Dr. William N. Redisch
NASA, GSFC
Code 701
Greenbelt, MD 20771

Mr. John P. Retzler
Nuclear S/V Manager
Applied Systems Eng. Dir.
5500 Canoga Avenue
Woodland Hills, CA 91367

Dr. Richard Reynolds
Dep. Dir., Defense Sci. Off.
Defense Advanced Research
Projects Agency
1400 Wilson Blvd.
Arlington, VA 22209

Mr. Clay Rogers
R & D Associates
P.O. Box 9695
4640 Admiralty Way
Marina Del Rey, CA 90291

Dr. Sven Roosild
Defense Advanced Research
Projects Agency
1400 Wilson Blvd.
Arlington, VA 22209

Mr. Carl Rosenberg
Boeing Aerospace Company
MS-2R-00
P.O. Box 3999
Seattle, WA 98124

Mr. Howard H. Sander
Sandia Laboratories
Division 2143, P.O. Box 5800
Albuquerque, NM 87185

Mr. Harry Schafft
Code A 327
National Bureau of Standards
Washington, DC 20234

Dr. Walter Shedd
Rome Air Development Center
ESR
Hanscom AFB, MA 01731

Dr. Joseph Srour
Northrup Res. & Tech. Ctr.
1 Research Park
Palos Verdes, CA 90274

Dr. E.G. Stassinopoulos
NASA-GSFC
Code 601
Greenbelt, MD 20771

Dr. C. Martin Stickley
The BDM Corp.
7915 Jones Branch Dr.
McLean, VA 22102

Mr. Fred Tietze
IBM Federal Systems Division
9500 Godwin Drive
Manassas, VA 22110

Dr. James H. Trainor
NASA, GSFC
Code 660
Greenbelt, MD 20771

Mr. Patrick Vail
RADC/ESR
Dept. of Electronic Tech.
M/S 64
Hanscom AFB, MA 01731

Dr. Victor Van Lint
Mission Research Corp.
1150 Silverado Street
La Jolla, CA 92038

Mr. R. Viola
Sperry Rand Corporation
Sperry Division
Marcus Avenue
Great Neck, NY 11020

Mr. Neil Wilkin
HDL
2800 Powder Mill Road
Adelphi, MD 20783

Dr. William Willis
TRW Incorporated
Defense and Space Systems Group
One Space Park
Redondo Beach, CA 90278

Mr. David S. Yaney
Bell Laboratories, Inc.
555 Union Blvd.
Allentown, PA 18103

Dr. James Ziegler
IBM
Thomas J. Watson Res. Ctr.
P.O. Box 218
Yorktown Heights, NY 10598

Internal to NRL

Dr. James H. Adams, Code 4020
Dr. Arthur B. Campbell, Code 6611
Mr. Charles Dozier, Code 6683
Dr. Charles S. Guenzer, Code 2004
Mr. Harold Hughes, Code 6816
Dr. John McElhinney, Code 6603-J
Dr. Martin C. Peckerar, Code 6814
Dr. Edward Petersen, Code 6611
Dr. Philip Shapiro, Code 6611 (50 copies)
Dr. Eligius A. Wolicki, Code 6601
Mr. J. C. Ritter, Code 6611
Dr. Keith Marlow, Code 6610
Dr. J. T. Schriempf, Code 6600
Dr. David O. Patterson, Code 6815
Code 2628 (20 copies)
Defense Technical Information Center (2 copies)

END

DATE

FILMED

9-82

DTIC